# HUMAN POWER

## TECHNICAL JOURNAL OF THE IHPVA

***NUMBER 50, SPRING 2000***



**Number 50**
**Spring 2000**

**$5.50**

# HUMAN POWER

Number 50 | Spring 2000 | $5.50/IHPVA members, $4.00



**HUMAN POWER**

is the technical journal of the International Human Powered Vehicle Association
Number 50, Spring 2000

**Editor**
David Gordon Wilson
21 Winthrop Street
Winchester, MA 01890-2851 USA
dgwilson@mediaone.net

**Associate editors**
Toshio Kataoka, Japan
1-7-2-818 Hiranomiya-Machi
Hirano-ku, Osaka-shi, Japan 547-0046
HQI04553@niftyserve.ne.jp

Theodor Schmidt, Europe
Ortbühlweg 44
CH-3612 Steffisburg, Switzerland
tschmidt@mus.ch

Philip Thiel, Watercraft
4720 - 7th Avenue, NE
Seattle, WA 98105 USA

**Production**
JS Design & JW Stephens

**IHPVA**
Paul MacCready, Honorary president
Chris Broome, USA, Chair
Ben Wichers Schreuer, The Netherlands, Vice-chair,
Open, Secretary/treasurer

**Publisher**
IHPVA
PO Box 1307
San Luis Obispo, CA 93406-1307 USA
Phone: +805-545-9003; hp@ihpva.org

*Human Power* (ISSN 0898-6908) is published irregularly for the International Human Powered Vehicle Association, a non-profit organization dedicated to promoting improvement, innovation and creativity in the use of human power generally, and especially in the design and development of human-powered vehicles.




## *IN THIS ISSUE*

**Bicycle chain transmissions**

Jim Spicer and his associates at Johns Hopkins have written a paper that will change minds, and design directions, on HPV transmissions. To give just one example: the losses associated with small sprockets on the rear wheel make "mid-drives" or countershaft gears suddenly attractive, and possibly hub gears too. They also find that chain lubrication doesn't seem to reduce losses: that will be even more controversial. (Your editor has high confidence in the data: he asked Chet Kyle, IHPVA founder and one of the foremost researchers in bicycle performance in the world, to look at them before publication. He had done a proprietary study on the same topic, and has produced broadly similar results.)

**Offset rims**

Vernon Forbes gives us another of his careful studies of spoked-wheel construction incorporating derailleur clusters or brake disks that cause the wheel to be "dished" (spoked asymmetrically). He shows that the use of rims that have off-center spoke holes brings about a considerable reduction in the difference in spoke tensions that otherwise makes highly dished wheels prone to spoke failure and occasionally to collapse.

**Rolling resistance**

John Lafford has tested, on equipment of his own design and construction, a prodigious number of bicycle tires, mostly of a size particularly suited to the front wheels of recumbent bikes. He measured rolling resistance and power loss over a range of speeds and inflation pressures. Jim Papadopoulos wrote a commentary on the results, and John Lafford responded, all in this issue.

**Power requirements for unfaired laid-back recumbents**

Bert Hoge and Jeroen Schasfoort wrote a short but valuable technical note in the beautifully produced Netherlands counterpart to *Human Power*: *HPV nieuws*. They showed, by testing a range of Dutch recumbent bikes, that the aerodynamic drag decreases as the angle of reclining increases.

**My propeller theory**

Gene Larrabee, whom *Human Power* named "Mr. Propeller" many years ago, summarizes his propeller theories and the developments that have resulted from them. He also pays tribute to those who inspired him and gave him the basic theories on which he built. Was Isaac Newton the first to state that we all stand on the shoulders of giants?

**Feet-on! review**

Mike Eliasohn writes a delightful review of what sounds to have been an equally delightful and truly interactive museum exhibit devoted to human power.

**Human power: the forgotten energy**

Your editor reviews a small fascinating book by Arnfried Schmitz, already well-known in these pages, on the origins of HPVs in France, on the characters of the protagonists, and (very modestly) on his own part in the revival of interest in these wonderful vehicles.

**Editorial from the Netherlands**

Ronald van Waveren, chair of the Netherlands HPV association, writes a guest editorial about the astonishing numbers of recumbent bicycles and HPVs in the Netherlands, and in particular about the annual celebration known as "Cycle Vision." Through delays in our publication we are too late to encourage you to visit this exciting event this year, but we hope that you will do so next year….

**Letters** include kind words from Chet Kyle; comments by Anil Rajvanshi on the publication of his article on rickshaws in the last issue (*Human Power* 49); and comments and corrections by Arnfried Schmitz on his article "Velocar variations", also in the last issue.

**CONTRIBUTIONS TO *HUMAN POWER***

The editor and associate editors (you may choose with whom to correspond) welcome contributions to *Human Power*. They should be of long-term technical interest. News and similar items should go to *HPV News* or to your local equivalent. Contributions should be understandable by any English-speaker in any part of the world: units should be in S.I. (with local units optional), and the use of local expressions such as "two-by-fours" should be either avoided or explained. Ask the editor for the contributor's guide (available in paper, e-mail and pdf formats). Many contributions are sent out for review by specialists. Alas! We cannot pay for contributions. Contributions include papers, articles, technical notes, reviews and letters. We welcome all types of contributions from IHPVA members and from nonmembers.



# On the efficiency of bicycle chain drives


***James B. Spicer,* Christopher J.K. Richardson, Michael J. Ehrlich and Johanna R. Bernstein***
***The Johns Hopkins University, Baltimore, Maryland 21218***
***Masahiko Fukuda and Masao Terada***
***Shimano Inc., Product Engineering Division, Sakai Osaka 590-77***



**ABSTRACT**

The efficiencies of bicycle drive trains have been studied to understand energy-loss mechanisms in these systems. An analytical study of frictional energy loss along with a series of experimental efficiency measurements of derailleur-type chain-drive systems under a range of power, speed and lubrication conditions are given to identify loss mechanisms. These measurements of mechanical efficiency are compared to infrared measurements performed during drive operation that show the heating of drive components resulting from frictional losses. The results of this study indicate that chain tension and sprocket size primarily determine chain-drive efficiency.


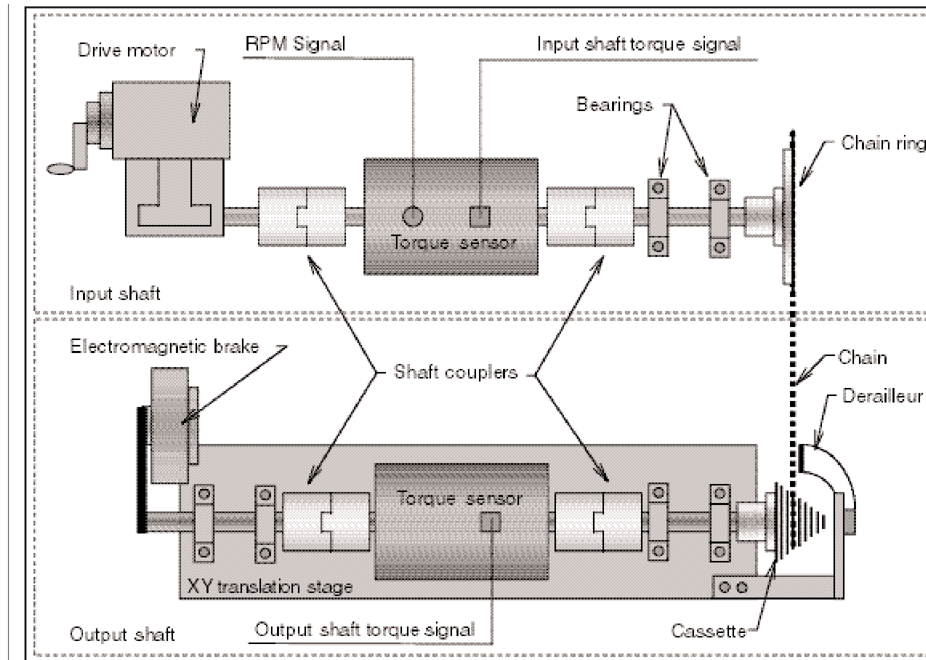


**Fig. 1. Experimental schematic of test stand showing elements of the drive assembly**

**INTRODUCTION**

When this study was performed, it was hoped that through identification of the loss mechanisms primarily responsible for limiting the efficiency of bicycle chain drives, methods for improving efficiency could be realized by eliminating or decreasing the various losses. Unfortunately, as will be shown, definitive identification of these mechanisms has not been successful. Rather, the results provide information on the efficiency of chain drives and, at the same time, lead to conclusions eliminating those mechanisms that do not dominate efficiency. We hope that the results here contribute to the overall body of work on chain-drive efficiency and also to the on-going discussion of this topic (Cameron 1999; Wilson 1999).

Even though design of chain drives is fairly well-understood (Vogwell 1994) the factors affecting efficiency have been considered only in passing as part of the design process. Generally design factors that are considered include chain length, load ratings, roller impact velocity, rotational forces, contact forces, chordal action and chain vibration (Tordion 1996). Since some of these are dynamic effects, the work presented here was conducted on chain drives during operation.

Hollingworth and Hills (1986a) performed a detailed theoretical and experimental study of chain contact forces during link articulation in heavy-duty chain drives and used these results to calculate the theoretical efficiency of chain drives assuming that frictional losses primarily affected efficiency (Hollingworth and Hills, 1986b). They found that the efficiency of the chain drive should increase with the number of sprocket teeth on each of the driver and driven sprockets. Unfortunately, no experimental results were given to verify their models.

In the work by Keller (1983) measurements of efficiency were made for different transmission systems (derailleur, internally geared hub, fixed), using chains exhibiting various conditions of repair (new, used, non-lubricated), under a variety of power-transfer conditions (Juden 1997). Without detailed analysis of Keller's results, it appears that they do not wholly support the idea that the efficiency is governed by friction. Work by Kidd, Loch and Reuben (1998) has attempted to quantify drive efficiency in relation to models of drive-train performance based on chain contact forces. While static measurements of these forces have agreed with models, efficiency-measurement results have not appeared in the literature (Kidd et al. 1996).

In this work, the efficiencies of bicycle chain drives are investigated both experimentally and theoretically to isolate factors associated with loss in these systems. A computer-controlled drive-train-testing system was designed to measure the performance of the chain, chain ring and rear cassette in a derailleur-type system. This system was used to measure chain-drive performance under a variety of operating conditions. Assuming that frictional forces degrade the overall efficiency of the system, simple analytical models for the losses of chain drives have been developed to estimate and identify the primary mechanisms of frictional loss. These models for drive losses have been used to interpret experimental results. Additionally, since losses due to friction ultimately are manifested as heating of the drive components, infrared images of the operating chain drive were taken.

## THEORY

If it is assumed that friction between contacting components performs work during drive operation, then power losses from the drive necessarily reduce efficiency. The normal force producing friction is related to the chain tension in the link during articulation and engagement. An analysis for this tension can be found in the work by Tordion (1996) and in the work by Kidd et al. (1998). Since the friction depends on chain tension, there are perhaps two major locations for loss in the drive that should be identified beforehand since the chain tension is large and is transferred from the chain to the sprocket at these locations. These include the surfaces between the inner link bushing and chain pin and between the sprocket tooth, link roller and inner link bushing. Rather than derive in detail the functional form for the losses, the results of models will be presented to give the reader a feeling for the anticipated results of experiment. The interested reader can find the full derivation elsewhere (Spicer et al. 1999).

### *Inner-link bushing and chain pin*

Since the chain tension is large on only one side of the drive, between the front chain ring and the rear sprocket, this loss has significant contributions only at two points. One of these is at engagement on the front chain ring and the other is at departure on the rear sprocket. Adding the contributions from these two points, the total work resulting from friction can be expressed as follows:

(1)

$$W_{f1} = \mu_1 \rho \left( \frac{\pi}{2} T_0 \right) \sum_{i=1}^{2} \sin(\varphi_i) 1n \left| \frac{1 + \tan(\alpha_i/2)/\tan(\varphi_i/2)}{1 - \tan(\alpha_i/2)\tan(\varphi_i/2)} \right|$$

where $\mu_1$ is the coefficient of friction at the pin/bushing interface, $\rho$ is the pin radius, $T_0$ is the free chain tension, $\varphi$ is the pressure angle (for new chains equal to $[35°–120°/N]$ where $N$ is the number of teeth on the sprocket), and $\alpha$ is the articulation angle (equal to $360°/N$). The subscripts on the angles refer to the front chain ring, 1, and the rear sprocket, 2. In deriving Eq. (1), it was assumed that the pin and bushing have a neat fit (all surfaces were assumed to be in contact) and that the coefficient of friction was a constant, independent of the chain tension.

The rate at which this work is performed represents the power loss resulting from friction, $P_f$. The average power dissipated per link by this source is written using the period of chain revolution (expressed in terms of the drive-sprocket angular frequency) along with Eq. (1). The resulting expression must be multiplied by the number of links in the chain to obtain the total power loss for this mechanism. The following result is obtained:

(2)

$$P_{f1Total} = N_1 \omega_1 W_{f1} / 2\pi$$

Note that the functional dependence of $P_{f1Total}$ on the articulation angle and, consequently, on the number of teeth on the drive and driven sprockets is not clear owing to the form of Eq. (1). However, if the number of teeth on the sprockets is large such that the articulation angles are small, $\tan(\alpha/2) \cong \alpha/2$, then the expression can be simplified such that the total power dissipated becomes:

(3)

$$P_{f1Total} \approx N_1 \omega_1 \mu_1 \rho \frac{\pi}{2} T_0 \left[ \frac{1}{N_1} + \frac{1}{N_2} \right]$$

A similar analysis can be carried out for the effects of chain offset with the result that the power lost as a result of offset has a form nearly identical to that given for friction at the pin-bushing interface except that a factor of the offset angle appears in the expression for offset losses. Since this angle is small, the frictional effects of offset should be small compared with pin/bushing losses. Any effect would necessarily appear in the largest offset conditions.

### *Sprocket tooth, link roller and inner link bushing*

A similar analysis for the losses at the tooth/roller/bushing interfaces can be performed with the following results:

(4)

$$P_{f2Total} = \mu_2 T_0 r_{Ri} \frac{N_1 \omega_1}{2\pi} \sum_{i=1}^{2}$$
$$\left[ \left( \frac{2\pi}{N_i} + \psi \right) \cos\varphi_i - \sin\varphi_i 1\mathrm{n} \left( \cos\left( \frac{2\pi}{N_i} + \psi \right) - \sin\left( \frac{2\pi}{N_i} + \psi \right) \cot\varphi_i \right) \right]$$

where $\mu_2$ is the coefficient of friction at the bushing/roller interface, $r_{Ri}$ is the inner radius of the roller, and $\psi$ is the roller rotation angle (the angle through which the roller executes no-slip motion on the tooth). Since the pressure angle depends on tooth number, a simplified form for the variation of the power loss with sprocket combination is difficult to obtain from Eq. (4).

Since both of these loss mechanisms involved friction between elements of the chain, it can be assumed that the coefficients of friction are approximately equal such that a total power loss can be written for the chain drive. This power loss is obtained by adding the losses given as follows:

(5)

$$P_{fTotal} = \mu T_0 \frac{N_1 \omega_1}{2\pi} \left\{ \frac{\pi}{2} \rho \sum_{i=1}^{2} \sin\varphi_i 1n \left| \frac{1 + \tan(\alpha_i/2)\cot(\varphi_i/2)}{1 - \tan(\alpha_i/2)\tan(\varphi_i/2)} \right| + \right.$$
$$\left. r_{Ri} \sum_{j=1}^{2} \left( (\alpha_j + \psi)\cos\varphi_j - \sin\varphi_j 1n \left| \cos(\alpha_j + \psi) + \cot\varphi_j \sin(\alpha_j + \psi) \right| \right) \right\}$$

where $\mu$ is the common coefficient of friction. It is noted that the total power loss per sprocket is reciprocally related to the tooth number if the roller angle vanishes. Using this expression for the total power loss where $N_1 = 52$, three separate configurations are examined and are given as follows:

Configuration A: $N_2 = 11$
Configuration B: $N_2 = 15$
Configuration C: $N_2 = 21$

These configurations were chosen to reflect situations that were realized experimentally in this study. Assuming that the roller angle is $\psi \cong 5.6°$ and also assuming that the geometrical pre-factors for each of the losses are approximately equal yields the following results:

(6)

$$\frac{P_{fTotalA}}{P_{fTotalC}} \cong 1.63 \quad \text{and} \quad \frac{P_{fTotalB}}{P_{fTotalC}} \cong 1.28$$



These results indicate that configuration A should have 63% more power loss than C and that configuration B should have 28% more power loss. For example, if a test of efficiency indicated a 5% power loss in configuration C, then configuration A should suffer an 8.2% loss and B should have a 6.4% loss.

## DESCRIPTION OF THE EXPERIMENTAL APPARATUS

To assess drive efficiency, a test stand was designed to measure the overall or average mechanical efficiency of the chain drive from the front chain ring to the rear transmission components. To assess the efficiency of the drive under various conditions, the power input to the front chain ring was measured and was compared to the power that was output by the rear drive sprocket. The ratio of the output power to the input power was used to quantify the overall efficiency of the system. To determine the powers in the drive and driven shafts, the torques transmitted by the shafts were measured along with the rotation rate of the drive shaft. Knowing the rotation rate of the drive shaft and the gear ratio, the rotation rate of the driven shaft could be calculated. The efficiency of the system was calculated using the following formula:

(7)

$$\%Efficiency = \frac{\tau_2 \omega_2}{\tau_1 \omega_1} \times 100\%$$

where $\tau_1$, $\omega_1$ are the torque and the angular frequency, respectively, of the drive shaft, and $\tau_2$, $\omega_2$ are the torque and the angular frequency of the driven shaft. To gather the data required for the efficiency calculations, the test stand was automated using computer control. The essential elements of the test stand are shown schematically in figure 1 (see page 3).

The drive shaft was driven by a variable-speed electric motor system connected to the drive shaft. The drive-shaft rotation rate from this system could be varied continuously under manual control. However, once the desired rotation rate was set, the rate was not actively controlled and the actual rotation of the drive shaft was measured using a speed sensor. The drive-shaft torque was measured using a rotary transformer torque sensor.

The chain drive was configured to the geometry found on bicycles with the distance between the front chain ring and rear cassette being adjusted by mounting the entire output-shaft assembly on a translational platform. Mounting the output drive components on this platform allowed for accurate adjustment of the cassette for distance and offset from the front chain ring. Additionally, the derailleur unit (Shimano® Dura Ace®) could be adjusted independently to satisfy recommended mounting conditions. The output shaft torque was measured using a second rotary torque sensor. The entire drive system was loaded using an electromagnetic brake mounted to the output shaft.

There are three signals that are recorded under computer control in a LabView®† programming environment: input and output torques and input rotation rate. The torque-sensor differential outputs were amplified using low-noise instrumentation amplifiers. Since the torque-sensor outputs were harmonically varying signals with amplitudes proportional to the torque, the signals were measured using lock-in techniques to improve the signal-to-noise of recorded signal amplitudes. To relate these signals to actual torque values, each of the torque sensors was calibrated using known static loads. By measuring the torque-sensor signals as a function of applied torque, a calibration curve was obtained that related signal level to the applied torque.

Finally, an infrared-camera system was used to acquire thermal images of drive components while the drive was in operation. Since frictional losses result in heating of the drive components, the infrared camera was useful in identifying those components that had the highest temperature rises. The primary component of this system is the infrared camera that operated with an InSb planar array sensitive in the 3–5 µm range. Again, using LabView software to control the camera and the image-acquisition-board operations, thermal images of the drive were acquired and stored for analysis and display. For these operations it was important to acquire images of the drive so that the drive component of interest occupied the same position in the infrared image from frame to frame. By acquiring images in this manner, the heating of an individual component, such as a single chain link, could be tracked accurately as a function of time.

## EXPERIMENTAL PROCEDURE

Four major areas for investigation were identified and were pursued.

*Time variation.* Measurements of efficiency were made over extended run periods (2 hours) to determine whether or not efficiency varied as a function of time during drive operation.

*Configuration.* Efficiency was mea-

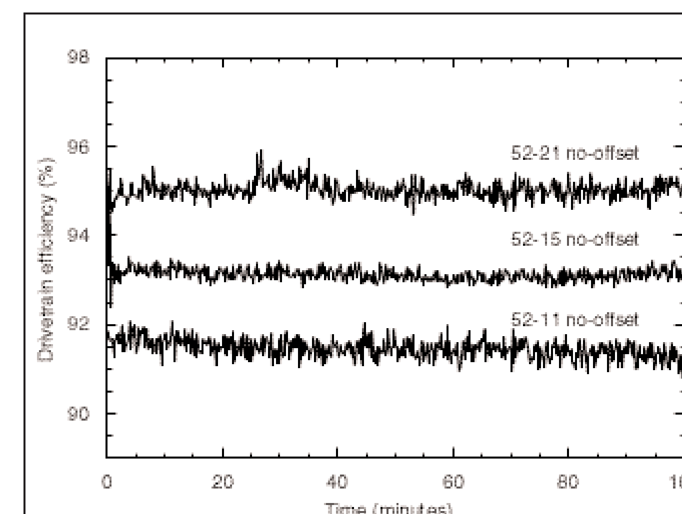


**Figure 2. Measured chain-drive efficiency as a function of time for three different drive configurations (52–11, 52–15 and 52–21) in the no-offset condition. Tests were run for two hours, but only the first 100 minutes are shown here. Note that efficiency is fairly constant during the entire time period.**

sured as a function of gear ratio (52–11 etc.) and the effects of offset were investigated to assess the effects of drive configuration.

*Power/rate.* Efficiency variations with input power and rotation rate were measured to determine if load or rate-dependent effects were present.

*Lubrication.* The effects of lubrication and de-lubrication on efficiency were quantified.

## EXPERIMENTAL RESULTS AND ANALYSIS

### *Time variation of efficiency*

A new chain used for these tests was cleaned using Simple Green™ Bike Cleaner/Degreaser and was lubricated using Generation 4: White Lightning™ self-cleaning lubricant. These tests lasted 120 minutes at 60 RPM 100W for each of the following chain-drive configurations: 52–11 no-offset, 52–15 no-offset and 52–21 no offset. As is shown in figure 2, the efficiency for all long-duration tests showed little-to-no long-term efficiency variations during the tests. The measured efficiencies for the three configurations are as follows:

| | |
|---|---|
| 52–11 no-offset: | 91.4% |
| 52–15 no-offset: | 93.2% |
| 52–21 no-offset: | 95.0% |

These values represent an average over the duration of the test. As a result of these long-duration tests, subsequent tests were run for no more than 30 minutes to assess efficiency or efficiency variations.

### *Configuration*

The next series of tests investigated the effect of chain configuration on efficiency. These tests lasted 30 minutes each and were conducted with the 52–15 combination in the no-offset condition. Consequently, the 52–11 and 52–21 combinations were tested in an offset condition as would occur for a properly configured bicycle. The results of these tests are summarized in Table 1.

First, comparing the results here with those in the long-duration tests, the effect of chain offset can be estimated. These data were obtained with the 52–11 and 52–21 configurations in the offset condition while those in the long-duration tests were taken with no offset. Comparing the data for 60 RPM 100 W tests shows that the offset lowers the efficiency by, at most, 0.5% when measurement precision is considered. Additionally, if the efficiencies are normalized by efficiencies measured in the 52–15 configuration (both sets of data were obtained with no offset), then it appears that the offset has a negligible effect on efficiency.

More importantly, in these mid-duration tests, the efficiencies show a consistent dependence on rear sprocket size where the larger the sprocket, the higher the measured efficiency regardless of the selected power or rotation rate. If the efficiency for 52–21 is 95.2% (as is found for 50 RPM 100 W), then the previous modeling results predict a difference in efficiency of 2.6% between the 52–21 and 52–11 combinations. From the data in the table, the measured difference between the 52–21 and 52–11 combination is 2.7%. These results indicate that the primary mechanism for chain-drive loss could be friction at the pin/bushing interface and friction at the bushing/roller interface.

### *Power and rotation rate*

To investigate the effects of power and rotation rate on drivetrain efficiency, more extensive measurements of efficiency under varying powers and rotation rates were completed. The chain was the same as that used in the other tests and the lubrication was not changed with measurements of efficiency being made sequentially at 5–8 minute intervals. All recorded values for efficiency have a precision (due to short-term noise) of ±0.2% and a long-term precision of ±0.3% under normal operating conditions.

Again, the efficiency results showed that higher efficiencies are obtained for those configurations that have larger sprockets in combination. It was also found that the efficiency decreases with increasing rotation rate for constant power input and that efficiency increases with increasing power for constant rotation rate. Both of these data trends can be related to the torque applied to the drive and ultimately to the chain tension. Analyzing the efficiency as a function of tension shows that the efficiency increases with chain tension regardless of input power or rotation rate. Additionally, for a given chain tension, the efficiency was found to be independent of drive rotation rate (between 40 and 80 RPM). The dependence of efficiency on chain tension is shown in figure 3 where the drive efficiency is shown as a function of the reciprocal chain tension.

This graph shows that for the tensions investigated in this study (76.2 to 305 N) that the reciprocal of the tension is linearly related to the drive efficiency. For each of the linear fits to the experimental data, the correlation coefficient exceeds 0.996. The extrapolated efficiencies at high chain tensions exceed 100% by a small amount (a few percent in the worst case).

**Table 1. Drive efficiencies for different chain configurations**

| | 50 RPM 100 W | 60 RPM 100 W | 70 RPM 100W | 60 RPM 150 W | 60 RPM 175W |
|---|---|---|---|---|---|
| 52–11 | 92.5 | 91.1 | 88.7 | 94.6 | 95.5 |
| 52–15 | 94.7 | 92.3 | 90.4 | 96.2 | 97.5 |
| 52–21 | 95.2 | 93.8 | 92.0 | 97.4 | 98.2 |

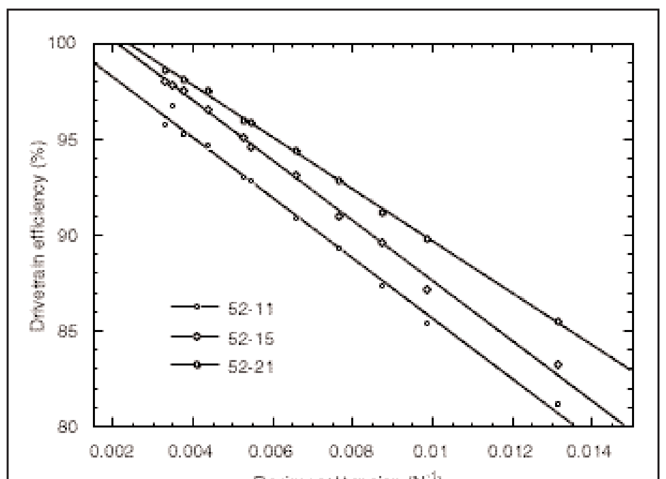


**Figure 3: Variation of chain-drive efficiency with the reciprocal of the chain tension. For this graph, chain tension has been calculated using the measured torque values and the radius of the front chain ring.**





Clearly, these data indicate that the fundamental operation of the drive must be related to the chain tension such that the efficiency increases with increasing tension even though the frictional losses should increase. This experimentally measured dependence of efficiency on chain tension can be explained only in a limited sense using the models for loss developed previously. For example, if the pressure angle changes with tension, then the calculated losses will vary with tension in a manner not considered previously. Measurements of link tension during articulation are currently being pursued using noncontacting optical measurement techniques to investigate these effects.

### *Lubrication*

In this phase of the study, the chain was thoroughly degreased/cleaned using commercially available degreasing agents (Castrol Wrench Force Degreaser™ and/or Simple Green™ Bike Cleaner/Degreaser) and was relubricated using one of three commercially available lubricants (Castrol Wrench Force Dry Lube™, Pedro's Syn Lube™ or Generation 4 White Lightning™).

The results in table 2 indicate that the previous trends for efficiency as a function of configuration and as a function of chain tension are still followed. However, these results also indicate that the actual lubricant used has little effect on the overall performance of the drive under laboratory conditions given the precision of the measurement. In addition, the chain used for the lubrication study was fully degreased and was re-tested for efficiency. This degreasing operation consisted of a five-minute scrub with kerosene followed by a cleaning with Castrol Degreaser. The measured efficiency of the de-lubricated chain for the 52–15 combination at 60 RPM and 100 W was 90.3% and at 200 W was 96.5%. These efficiencies are essentially the same as those measured for the chain in the re-lubricated condition.

### *Infrared measurements during chain-drive operation*

Infrared images of the chain drive during operation aid the interpretation of the efficiency measurements that have been presented and also support aspects of the modeling of chain-drive loss since frictional losses should heat the drive components. Simply put, the chain components responsible for mechanical loss should heat the chain and cause its temperature to rise. Since the average heat deposition rate equals the average mechanical power loss, the heating should have a functional dependence similar to that found for frictional losses.

To acquire infrared images, the chain drive was set initially to a low rotation rate and the components were allowed to reach a steady state in this mode of operation. The rotation rate and brake resistance were then increased rapidly to achieve the desired rate and power settings (100 W 60 RPM, etc.). Infrared image acquisition began prior to (or during) the time of power and rotation increase. Images were acquired at set time intervals (e.g., approximately 30 seconds) for the duration of the test such that actual image acquisition occurred synchronously to a particular link in the chain. Since pixel intensity is proportional to the infrared energy reaching the detector and the amount of infrared emission is proportional to the temperature of the component, the pixel intensity is directly proportional to temperature. This method for data acquisition allows the temperature

**Table 2. Efficiencies for different drive rotation rates and sprocket configurations (input power 100W)**

**2.1 Castrol Dry Lube™**

| | 40 RPM | 60 RPM | 80 RPM |
|---|---|---|---|
| 52–11 | 92.8 | 89.4 | 84.2 |
| 52–15 | 94.0 | 90.9 | 86.5 |
| 52–21 | 95.2 | 92.0 | 88.3 |

**2.2 Pedro's Syn Lube™**

| | 40 RPM | 60 RPM | 80 RPM |
|---|---|---|---|
| 52–11 | 93.6 | 89.9 | 85.6 |
| 52–15 | 95.6 | 92.6 | 88.8 |
| 52–21 | 95.3 | 92.6 | 89.0 |

**2.3 Generation 4 White Lightning™**

| | 40 RPM | 60 RPM | 80 RPM |
|---|---|---|---|
| 52–11 | – | – | – |
| 52–15 | 94.2 | 91.1 | 87.2 |
| 52–21 | – | – | – |

**52–21: 60 RPM, 150W**

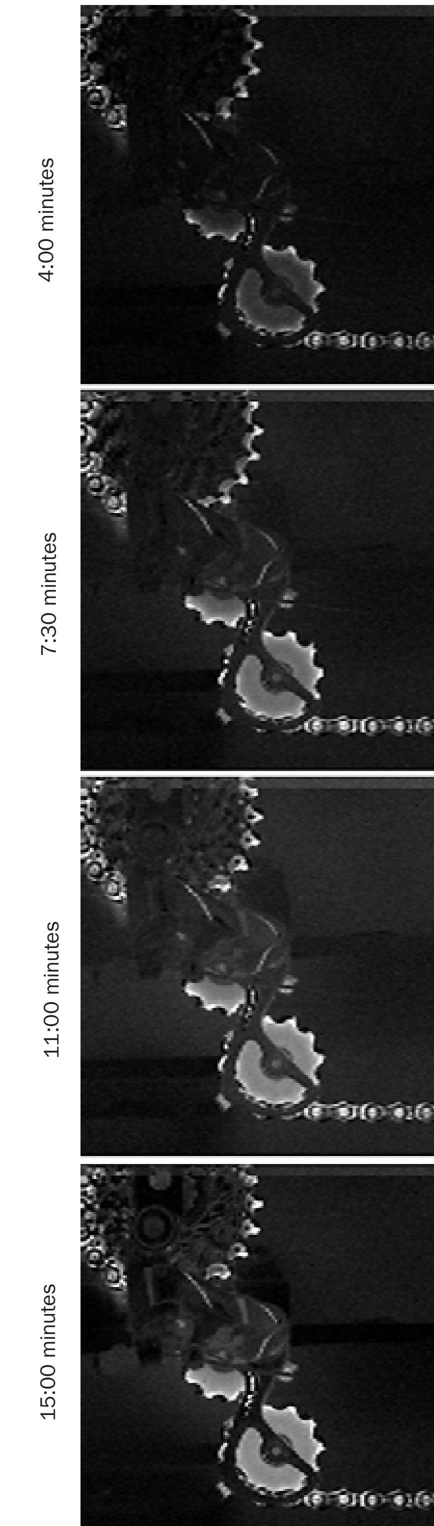


**Figure 4: Infrared images of chain drive during operation showing effects of frictional heating.**

increases in various components to be mapped as a function of time after imposition of the heat load.

Representative results are shown in figure 4 where a series of four infrared images from efficiency tests for the 52–21 configuration are shown. At the beginning of the test, the infrared images showed only variations of emissivity since all components were in thermal equilibrium. From these images (taken at the times indicated) various qualitative observations are given as follows.

1. The chain pins rapidly heat on the radial surfaces and reach near steady-state temperatures within 4–5 minutes.
2. At high chain tensions and low rotation rates, both the guide and the tension pulleys heat primarily from the chain.
3. Steady-state temperature conditions for the chain drive are established within approximately 15 minutes after the beginning of a test.

These observations are in general agreement with the proposed frictional-loss mechanisms. The rapid heating at the radial pin surfaces is consistent with heating at the pin-bushing interface. At low chain tensions, the frictional losses should be relatively low and the temperature rise in the chain should be low. At high chain tensions and low rotation rates, the frictional losses in the chain should be relatively high producing large temperature rises in the chain. The pulley-bearing losses should be relatively low. Even though the infrared images provide a wealth of qualitative information, quantitative analysis of chain-drive heating must be performed using the temporal evolution of pixel intensity.

In Fig. 5 the infrared pixel intensity for positions on a chain pin, on a pulley tooth and on the body of the pulley (midway between the bearing and the pulley teeth) are shown as a function of time for different input powers. These data were taken at 60 RPM in the 52–21 configuration. These results clearly show that the chain pin rises in temperature more rapidly than the other locations regardless of the input power and indicate that heating results from frictional losses near the pin.

The data for the chain and the pulley tooth indicate that the component temperature rises with the input power. For the pulley tooth, at 50 W input power, the maximum pixel value is approximately 23 units; at 100 W, 35 units and at 150 W, 65 units. These results are in rough agreement with the loss models presented previously where the frictional losses are directly proportional to the input power.

Unfortunately, the power loss in each of these cases is not proportional to the input power owing to the dependence of efficiency on chain tension. Using measured values for efficiency under the conditions for the data in Fig. 5 (97.2% for 150 W, 94.4% for 100 W and 85.5% for 50 W) indicates that 4.2 W of power were lost at 150 W input; 5.6 W at 100 W input and 7.3 W at 50 W input. Obviously, for a lower power loss, the temperature rise should be lower if the lost power is converted entirely to heat by frictional loss. It would be expected that the temperature rise would be lowest for the 150 W input test since the measured power loss is lowest for this case.

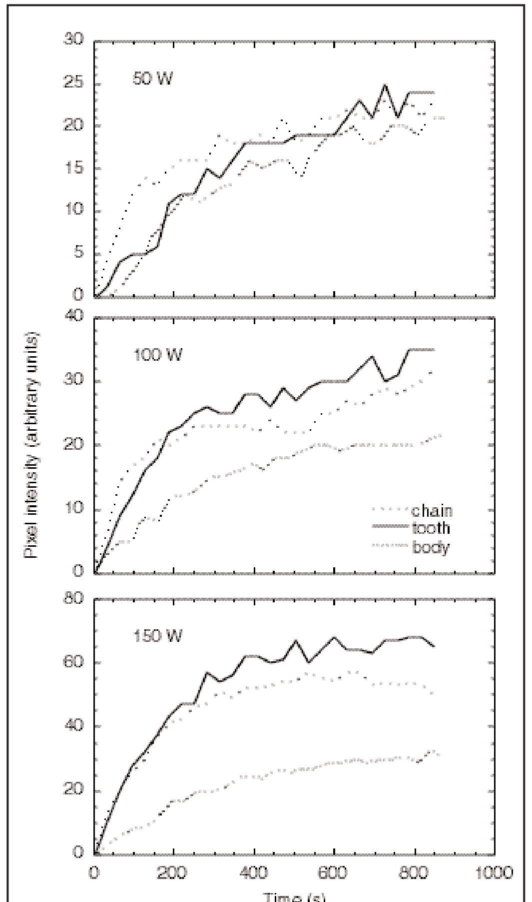


**Figure 5: Variation of infrared emission with time during chain operation for different drive components. At time equal to 0 s, the chain drive was placed under full power loading.**

## DISCUSSION AND CONCLUSIONS

Tests of efficiency for the derailleur-type chain drive indicate that the overall efficiencies for the transfer of power from the front drive sprocket to the rear sprocket range from 80.9% to 98.6% depending on the conditions of drive operation. Primary factors affecting the efficiency include the sizes of the sprockets in the drive and the tension in the chain.

It was found that larger sprockets provide more efficient transfer of power while smaller sprockets proved to be less efficient. Simple, frictional loss models were developed that gave sprocket-size loss variations that agreed with those variations measured experimentally. Typically, a 2–5% loss difference was measured between the 52–11 and the 52–21 sprocket combinations depending on the drive operating conditions.

Experimental results indicated that the efficiency of the chain drive varied as a function of chain tension. It was found that the efficiency varied linearly with the reciprocal of the average chain tension with the highest efficiencies occurring at high chain tensions and lowest at low chain tensions. For example, the highest efficiency measured in the study, 98.6%, was measured at a chain tension of 305 N and the lowest, 80.9%, at 76.2 N.

It was found that chain-line offset and chain lubrication have a negligible effect on efficiency under laboratory conditions. Calculations of frictional loss resulting from offset indicate that this loss should be small compared to those produced by other mechanisms. This was verified experimentally. Lubrication effects on chain efficiency were tested using three different chain lubricants under a variety of test configurations. No significant quantifiable effect of lubrication could be inferred from these tests.

Infrared measurements of drive components indicate that frictional losses in the chain cause the chain temperature to rise during operation. This increase in temperature did not correlate with measured efficiencies under various conditions of operation. Infrared measurements on lubricated and delubricated chain links showed that the frictional heating did not depend on lubrication.

From the results of this study, it appears that the efficiency of the bicycle chain drive depends intimately on the chain operation as it engages and departs from the sprockets on the high-tension part of the drive. Owing to the high efficiencies measured under high chain tensions, friction can account for only a few percent of the overall losses. Most probably, mechanical losses that are not converted to thermal energy in the drive account for the remainder of the measured loss.

## NOTES

†LabVIEW®, National Instruments Corporation is a computer software program useful for running scientific instruments by computer. National Instruments Corp. See http://www.ni.com/labview for vendor information.

## REFERENCES

Cameron, A. 1999. Measuring drive-train efficiency, *Human Power* 46:5–7.

Hollingworth, N.E., and D.A. Hills. 1986a. Forces in heavy-duty drive chain during articulation. Instn Mech. Engrs, 200:C5, 367–374.

Hollingworth, N.E., and D.A. Hills. 1986b. Theoretical efficiency of cranked link chain drive. Instn Mech. Engrs, 200:C5, 375–377.

Juden, C. 1997. Measurements of efficiency of chain and shaft drives. http://www.soroos.net/hbs/chains/sn1_2_2.html, (1997).

Keller, J. 1983. Der Wirkungsgrad im Fahrradantrieb. *Radmarkt*, 12:71–73.

Kidd, M., N. Loch, and R. Reuben. 1996. Bicycle chain efficiency. *The Engineering of Sport*, S. Haake, ed. Rotterdam: Balkema, 217–220.

Kidd, M., N. Loch, and R. Reuben. 1998. Experimental investigation of bicycle chain forces. Submitted to *Experimental Mechanics*.

Spicer, J., M. Ehrlich, J. Bernstein, C. Richardson, M. Fukuda, and M. Terada. June 1999. Efficiency and energy loss location in bicycle chain drives. Submitted to the *Journal of Mechanical Design*.

Tordion, G.V. 1996. Chains. *Mechanical design handbook*. H.A. Rothbart, ed. McGraw Hill, 25.1–25.12.

Vogwell, J. 1994. Chain drives. *Rotary power transmission design*. K. Hurst, ed. McGraw-Hill Europe, 79–95.

Wilson, D.G.1999. Transmission efficiency, *Human Power* 48:20–22.

———

**Corresponding author:*
*James B. Spicer, Associate Professor*
*Dept. of Materials Science & Engineering*
*The Johns Hopkins University,*
*3400 N. Charles St., Room 102*
*Maryland Hall,*
*Baltimore, MD 21218, USA*
*spicer@jhu.edu; 410-516-8524*

*The Hopkins group pursues work in pulsed and ultrafast (femtosecond) laser-based materials processing and characterization. In contrast, the expertise of the Shimano participants leans towards the design and manufacture of cycling components. All of the authors express their gratitude to the Baltimore Orioles for the use of Camden Yards where many fruitful technical discussions about this work were held.*

## SUMMARY OF EQUATIONS

1 $$W_{f1} = \mu_1 \rho \left(\frac{\pi}{2} T_0\right) \sum_{i=1}^{2} \sin(\varphi_i) 1n \left| \frac{1+\tan(\alpha_i/2)/\tan(\varphi_i/2)}{1-\tan(\alpha_i/2)\tan(\varphi_i/2)} \right|$$

2 $$P_{f1Total} = N_1 \omega_1 W_{f1} / 2\pi$$

3 $$P_{f1Total} \approx N_1 \omega_1 \mu_1 \rho \frac{\pi}{2} T_0 \left[\frac{1}{N_1} + \frac{1}{N_2}\right]$$

4 $$P_{f2Total} = \mu_2 T_0 r_{Ri} \frac{N_1 \omega_1}{2\pi} \sum_{i=1}^{2} \left[\left(\frac{2\pi}{N_i} + \psi\right)\cos\varphi_i - \sin\varphi_i 1n\left(\cos\left(\frac{2\pi}{N_i} + \psi\right) - \sin\left(\frac{2\pi}{N_i} + \psi\right)\cot\varphi_i\right)\right]$$

5 $$P_{fTotal} = \mu T_0 \frac{N_1 \omega_1}{2\pi} \left\{ \frac{\pi}{2} \rho \sum_{i=1}^{2} \sin\varphi_i 1n \left| \frac{1+\tan(\alpha_i/2)\cot(\varphi_i/2)}{1-\tan(\alpha_i/2)\tan(\varphi_i/2)} \right| + r_{Ri} \sum_{j=1}^{2} \left((\alpha_j + \psi)\cos\varphi_j - \sin\varphi_j 1n \left|\cos(\alpha_j+\psi) + \cot\varphi_j \sin(\alpha_j+\psi)\right|\right) \right\}$$

6 $$\frac{P_{fTotalA}}{P_{fTotalC}} \cong 1.63$$
and
$$\frac{P_{fTotalB}}{P_{fTotalC}} \cong 1.28$$

7 $$\%Efficiency = \frac{\tau_2 \omega_2}{\tau_1 \omega_1} \times 100\%$$

# Offset rims reduce the amount of dish

*by Vernon Forbes*


**ABSTRACT**

*Offset rims reduce the amount a rear wheel is dished. Two offset rims are tested and the results compared to a standard rim. Possible implications are discussed.*


**INTRODUCTION**

"Dish" in a bicycle wheel is a measure of its lack of symmetry. Usually this is given as a ratio of two lengths (defined later). Sometimes dish is also expressed as the ratio of, and as the difference of, the average spoke tensions on the drive side and the non-drive side of the hub. An undished wheel is one with the rim centered over the midpoint of the axle, not of the hub. In a front wheel, the rim is centered over both the axle and the hub. When viewed straight on the front wheel's rim can be seen to fall in the middle of the front hub, to rest equally between the flanges. A front wheel that is not centered on the axle cannot be centered in the frame or between the brake blocks.

In the rear wheel the rim is centered over the axle; it is not centered over the hub. This is the awkward solution to the problems posed by the development of the derailleur. Before the development of derailleurs both the front and rear wheels were centered over the hubs. With the development of derailleurs came multiple-cog freewheels which presented the problem of how to accommodate the additional cogs. Bicycle designers could do one of three things. For one, they could spread the stays and widen the rear axle to make room for the freewheel block. If they did this the bottom bracket would have to be widened also to keep the chain in line with the freewheel. Many consider wider bottom brackets harder to pedal. Their other choice was to center the rim over a very narrow hub. They could move the hub flange on the left side in by the same amount the freewheel block moved the right side hub flange in. However, wheels built with narrow hubs are laterally weaker than wheels built with wide hubs. The idea they hit upon was a compromise; they spread the rear dropouts a little and narrowed the rear hub a little so they could move the whole hub over between the dropouts to make room for the freewheel.

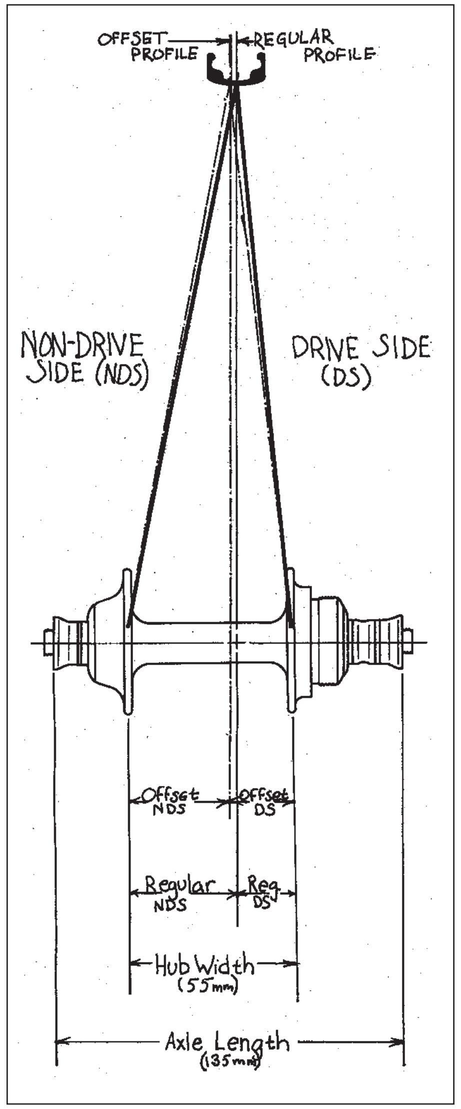


**Figure 1. Wheel cross-section for symmetric rims (after Brandt) with modifications for asymmetric rims.**

One effect a freewheel has is to increase spoke tension on the right, or drive side (DS) relative to the left, or non-drive side (NDS). The ratio of DS/NDS measures what is commonly referred to as dish. In this ratio the two distances are those from the plane of the rim centerline to the outside surfaces of the hub flanges. Increased freewheel width increases the severity of dish. The newer eight-speed freewheels require more dish than did older five speeds. Increased dish results in DS spokes being tighter. Cyclists are long familiar with the increased tendency for spokes to break on the freewheel side (Forbes 1998–99). One spoke manufacturer recommends 785-1079 N (176–243 lbf) spoke tension for the DS.[1] This is well below the threshold for failure, established by Brandt as 2649 N (595 lbf) for lighter spokes and 3139 N (706 lbf) for heavier spokes (Brandt 1983). Another spoke manufacturer specifies which hub to use and recommends the DS be tightened to 1079 N (243 lbf) and the NDS be tightened to 883 N (199 lbf). (This has the DS 22% tighter than the NDS.[2]) While this is a moderate amount of dish perfectly adequate for most applications it does not allow for differences in the amount of dish required resulting from hubs with different freewheel widths, axle lengths and distance between a hub's flanges. These are properties of the hubs and since it is rare for two hubs to have the same measurements no one can specify the tensions on each side of the wheel unless s/he also specifies which hub to use. Shraner (1999) gives the following tension recommendations for wheels with "normal rims". He recommends 900–1000 N (202–225 lbf) of tension for "normal rims" in the front wheel and in the rear wheel he recommends 600–700 N (135–157 lbf) for the NDS and between 1000–1100 N (225–247 lbf) for the DS (this has the DS between 57–66% tighter than the NDS; Schraner 1999). However, he does not specify which hub must be used to achieve this range of ratios.

Unequal spoke tension caused by rear-wheel dish has caused some manufacturers to experiment with previously rejected solutions. To make room for the wider freewheels some manufacturers have used longer rear axles. However, this changes the chainline and unless the bottom bracket is also widened it can result in difficult shifting and premature chain wear. Another solution to the problem of the DS being at a higher tension than the NDS is to use a "dishless" hub. A "dishless" hub must be a narrower hub. It has the NDS flange moved in closer so that it is the same distance from the rim center as the DS flange. However "dishless" hubs that are wider are known to be laterally stronger than narrow, dishless hubs.



Recently, offset rims (Ritchey, Bontrager) have been developed that have the spoke holes offset closer to the NDS (see figure 2). Both sides of the wheel are affected equally: the DS spokes are put at a steeper angle as the NDS spokes are put at a shallower one (see figure 1). This equalizes tension, reducing the failure rate of spokes on the DS due to fatigue. The ability of these rims to reduce the amount of dish is tested below.

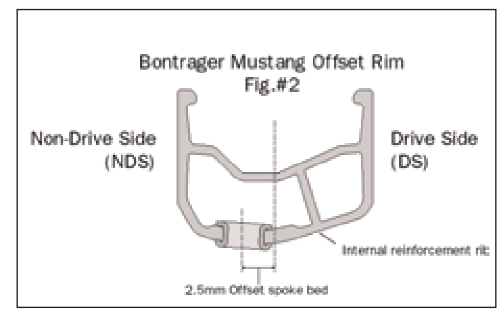


**Figure 2. Offset rim: Bontrager Mustang (reproduced here with permission).**

**METHODS**

Three 26x1.75 32-spoke rims were tested, two offset and one non-offset, for comparison. The offset rims were a Ritchey OCR (Off-Center Rim) and Bontrager Mustang Asym (Asymmetrical). The non-offset rim was a Matrix Singletrack. Each of these rims was built up 3X on a 32-spoke low-flange Suntour XC Pro hub with a 45-mm flange diameter, or spoke circle (measured center-to-center) using DT stainless-steel 14g spokes, 264-mm long. The Suntour hub measured 55 mm between flanges, center-to-center (see figure 1). The 55-mm distance was chosen because it was midway between the distances measured in a previous article. (The average for a 7-sp hub was 58.4 mm and the average for an 8-sp hub was 55.3 mm between the flanges, center-to-center; Forbes 1998–99). A 135-mm axle length, locknut-to-locknut (see figure 1) was used at all times. Each wheel was tested at two different levels of dish approximating the mean freewheel thicknesses of 7-sp (44.5 mm) and 8-sp (48.0 mm) freewheels established previously (*Ibid.*). Dish was changed by moving spacers from one side of the axle to the other and redishing the wheel, e.g., the axle was first spaced for a 7-sp spacing on a 135-mm axle. The wheel was then dished using a Wheelsmith dishing gauge. The Ritchey OCR was the first to be built up and tested. A rim transfer for all subsequent rims used the same hub and spokes.

Previously we had suggested that wheel dish could be predicted from a hub's measurements which we expressed as a ratio (DS/NDS). To measure dish on wheels that are already built up we are expressing dish as the difference in spoke tension between the DS and the NDS (DS–NDS). All tension measurements were taken with a Wheelsmith spoke tensiometer. At each level of dish the wheel was measured at three levels of tension corresponding, e.g., to tensiometer readings of 75, 80 and 85 for the DS. A copper template insured that tensiometer readings were taken 30 mm from the rim edge. Each reading was taken twice. If the two readings did not agree a third reading was taken. If there was any doubt about the reading on a spoke the procedure was repeated until a true reading was taken. After one level of dish was tested at three levels of tension the axle was respaced and the process repeated for the remaining levels of dish. Each level of dish was established using a 135-mm-long axle (locknut-to-locknut) as the overall length.

**RESULTS**

The chief interest for us was the difference in tension between the DS and the NDS. The mean spoke tension for each side of the wheel was first determined. Tension here is expressed as nominal tensiometer readings, not as Newtons or poundals. To measure dish the tension on the NDS (which was presumably less tight) was subtracted from the tension on the DS to determine the difference in tension. The accompanying figure (see figure 3) shows the tension differences between the DS and the NDS for two levels of dish corresponding to the mean 7-speed and 8-speed spacing. The two levels of dish are expressed in mm and measure the distance from the outside edge of the locknut on the DS to the flange center. Table 1 summarizes the data in figure 3. For both figure 3 and table 1, freewheel width (F/W width) is measured as the DS locknut-to-flange center in mm.

**DISCUSSION**

Figure 3 plots dish as differences in spoke tension between the drive side and the non-drive side (DS-NDS). The graph plots three lines; one for a Bontrager Asym, a Ritchey OCR, and a standard non-offset rim. A front wheel,

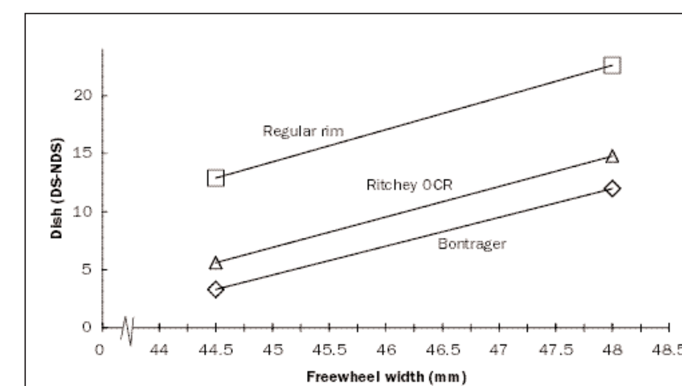


**Figure 3. Tension differences (dish) for regular and offset rims.**

**Table 1. Tension differences (DS-NDS)**

| # speeds | F/W width | Reg | OCR | Asym | % reduction OCR | % reduction Asym |
|---|---|---|---|---|---|---|
| 7-sp | 44.5 | 12.9 | 3.3 | 5.6 | 74% | 57% |
| 8-sp | 48.5 | 22.6 | 12.0 | 14.8 | 47% | 35% |

or any wheel with no dish would plot a value at zero. The higher the number the more severely a wheel is dished. Less dish is desirable. What is obvious is that the non-offset rim has the greatest tension differences, for all levels of dish. Both the offset rims show a significant reduction in dish. While both offset traces are below the standard rim trace, the Ritchey rim trace is below the Bontrager rim trace.

There exist a number of differences between these two rims which may explain our findings. Bontrager advertises his rims as having 2.5 mm of offset,[3] while Ritchey ads used to claim a 3-mm reduction in dish; they currently advertise a 50% reduction in dish.[4] One possible explanation is rim width. Our measurements showed the Bontrager Mustang was 21.8 mm wide and the Ritchey Rock OCR was 24 mm wide. With a wider rim you can move the spokes further over to the NDS. While the Bontrager rim is 2.2 mm narrower it has only 0.5 mm more dish than a Ritchey. There is a weight penalty for a wider rim. We measured the Bontrager at 415 g (he advertises 430 g) and the Ritchey at 484 g. Wider rims are laterally stronger. In terms of height the Ritchey advertises 12 mm height and the Bontrager advertises 13 mm height. Deeper rims are radially stronger. Both rims are made from 6061-T6 aluminum alloy.

Offset rims have been criticized by some as being weaker because they lack ferrules, or "spoke sockets" that join the upper and lower parts of a box-section rim so the spoke pulls on both sections of the box-section rim. In answer to this both rims come with "internal reinforcements". Figure 2 depicts a rib which joins the top and bottom as did Wilderness Trail Bikes (WTB) in its PowerBeam rim. Bontrager rims use one rib ("dual cavity" or double box) while Ritchey rims currently use two ("triple box"). The ability of internal reinforcing ribs to act like a ferruled rim is unclear. While we cannot be sure if our Ritchey OCR is triple box or not it would help explain why the Ritchey is nearly 70 g heavier. This is in light of the fact that while the Bontrager is eyeletted the Ritchey is not.

The graph illustrates that for all freewheel thicknesses, offset rims give a dramatic reduction in dish, as measured as tension differences. Because the Ritchey yields lower values presumably the spoke holes are more offset. Although both offset rims reduced dish compared to the standard rim the Ritchey had slightly lower tensiometer readings. Compared to the Bontrager rim, the Ritchey readings were 2.3 lower for 7-sp spacing and 2.8 lower for 8-sp spacing rim. This, however, may be due to the Ritchey's being a wider and heavier rim.

## DISH AS HUB MEASUREMENTS

Several claims are made for Ritchey OCR rims. One of them is that the Ritchey OCR rim will reduce dish from 6 mm to 3 mm using a Ritchey hub; a 50% reduction. We previously found that the dish on most hubs is considerably more than 6 mm. We surveyed the same 74 hubs we did in a previous study (Forbes 1998–99).

Table 2 summarizes the actual average amount of dish expressed as distance measurements for 74 hubs with a 55-mm-wide hub on a 135-mm axle we previously examined.
We see from the table that actually the Ritchey OCR would reduce dish from 9 mm to 6 mm on a typical 7-speed and from 17 mm to 14 mm on a typical 8-speed. These were reflected in lower tension differences. Inspection of table 1 reveals that when compared to a conventional rim, the Ritchey OCR rim yielded a 9.6 smaller difference in tensiometer readings for 7-sp spacing, (a 74% reduction) and a 10.6 difference in tensiometer readings for 8-sp spacing, (a 47% reduction).

## CAUSES OF DISH

The utility of these rims may be especially suited to wide rear hubs. Previously we noted how dish is the result of several variables (*Ibid.*). For any given freewheel both freewheel thickness and hub width contribute to dish in different ways.

Consider the effects of both freewheel thickness and hub width on dish. Increasing the freewheel thickness moves the entire hub over to make room for it. This pushes the DS flange in closer to the rim center as the NDS flange is pushed further from the rim center. By comparison, increasing the hub width affects dish by pushing the NDS flange further away from the rim, leaving he DS flange alone. Because freewheel thickness affects both flanges and hub width affects only one flange we view freewheel thickness to affect hub dish at twice the rate of hub width. It is for this reason that we have suggested that increasing hub width was not half as bad as increasing freewheel width.

The ability of an offset rim to attenuate dish depends on the source of the dish. Because offset rims affect spokes on both flanges an offset rim would reduce freewheel-induced tension differences at the same rate as the freewheel causes them. By comparison, hub-width-induced tension differences affect only one flange and offset rims attenuate dish by affecting both flanges. We would expect for offset rims to reduce hub-induced dish at twice the rate caused by hub width. Offset rims would be twice as effective in attenuating hub-induced dish as they are in attenuating freewheel-induced dish. That said, it is reasonable for offset rims to make for an increased widespread application of wider hubs, with all the benefits of increased lateral strength.

Offset rims may find an additional application for offsetting front-wheel dish induced by disk brakes. During the preparation of this article both Ritchey and Bontrager each introduced rims for use with a front disk brake. Interestingly, the Ritchey front OCR is 24 mm wide, the same width as the Rock OCR we tested which is no longer made. Unlike the Rock OCR, it does not appear to have any internal reinforcing ribs and is eyeletted. Phil Wood is listed as offering a front hub threaded to accept a disc brake in both a dished and undished versions (Sutherland 1995). Looking at their dimensions it appears that the undished hub has a narrower hub shaft (flange-to-flange) than the dished hub. If it is for a dished front wheel then using an offset rim would be an ideal solution. The Ritchey literature used to claim a 3-mm reduction in dish for their rear wheel. Dished models of Phil Wood front-brake hubs threaded for a disk brake are dished between 2–13 mm, depending on the front axle length (locknut-to-locknut). Only two hubs had 2 mm dish and the other eight were 3 mm or more. The Sturmey-Archer BFC drum brake is dished 4 mm. We can think of no more appropriate a use for an offset rim than for a front wheel with a disc or drum brake. We have examined the benefits of offset rims in reducing rear-wheel dish only.

**Table 2. Dish measured as distance difference (DS-NDS)**

| # speeds | F/W width | Center to DS | Center to NDS | Difference (DS-NDS) Standard (DS-NDS) | OCR (DS-NDS) | Asym (DS-NDS) |
|---|---|---|---|---|---|---|
| 7-sp | 44.5 | 23 mm | 32 mm | 9 mm | 6 mm | 6.5 mm |
| 8-sp | 48.5 | 19 mm | 36 mm | 17 mm | 14 mm | 14.5 mm |





## BENDING-MOMENT ASYMMETRY

It is natural, however, to assume that if form follows function we would expect to be able to see the symmetry and balance reflected in force-balanced structures. In offset rims the spoke holes are drilled closer to one side. One cannot help but suspect for such a glaring asymmetry to somehow reflect an underlying unequal distribution of force, or lack of balance.

Offset rims have what can be called bending-moment asymmetry. N.B.: we make the distinction between vertical, or up-and-down bending moment and lateral, or side-to-side bending moment. The longer DS half of the rim the more bending-moment it has. The shorter the NDS half of the rim the less bending-moment it has so that a vertical load, from, e.g., sitting on a bicycle, exerts more vertical bending-moment to the DS than the NDS side of the rim.

One possible effect of this is that every bump in the road would deform the longer DS more than it did the shorter NDS, relative to the centerline. That said, any vertical loading will result in the rim having increased DS bending movement. At the very least this might result in increased denting ("flat spots") of the DS half of the rim during cornering.

Vertical loads are thought to loosen the bottom most spokes making them likely to become unscrewed. Another possible effect of bending-moment asymmetry is that any vertical load will bend the rim on the DS and the spokes the DS might loosen more and their nipples be more likeley to unscrew. The wheel might be more likely to get out of true. Cornering, on the other hand, can subject the wheel to lateral loads. Right-hand bicycle turns increase the tension on the DS spokes in "tension peaks" as the wheel rotates while it leans into a turn. Now if the rim on the DS were also to experience some additional vertical bending in response to cornering then that would tend to loosen the spokes. So the "tension peaks" caused by lateral loading might be offset by any tension losses as a result of vertical loading. Brandt (1983) has suggested that fatigue is the result of the interaction between peak and baseline tension in a tension cycle. If this were so then we might expect that an offset rim might reduce the frequency of DS spoke failure in two ways. First, it would equalize spoke tension thus decreasing the baseline tension in DS spokes. Second, it would reduce the tension "peaks" experienced by the DS spokes during right-hand turns due to lateral movement because of the rim's increased complementary vertical bending movement during cornering.

However, this is all highly speculative. The possible effects of bending-moment asymmetry in offset rims are not known. Possible effects include the increased likelihood of rim dents on the DS as well as spokes unscrewing on the DS due to vertical movement and a decreased incidence of fatigue failure due to vertical movement attenuating stress peaks caused by lateral movement during cornering.

Despite our attempts to limit or control for tension differences, measurement error cannot be ruled out. We found that even differences as small as 0.5 mm in axle spacing would affect tensiometer readings.

## CONCLUSIONS AND RECOMMENDATIONS

Offset rims were found to significantly reduce rear-wheel dish for both 7-sp and 8-sp spacing. The rims have additional application in reducing front-wheel dish induced by hub brakes.

## NOTES

1. Wheelsmith tensiometer: a professional wheelbuilding device for exact spoke-tension measurements [pamphlet; 1989]. Menlo Park, CA: Wheelsmith Fabrications, Inc. The pamphlet comes with the tensiometer, although it does not give a NDS tension recommendation. For more information, Wheelsmith Fabrications, Inc., 3551 Haven Ave., Ste. R Menlo Park, CA 94025-1009 Telephone: 415-364-4930
2. *Mastering the art of wheelbuilding.* 1996. DT Swiss Bike Technology USA and Campagnolo. Certification seminar brochure. Extreme Skills Seminars and Extreme Exposure Promotions. Grand Junction, CO: LLC, p. 11.
3. Bontrager components nineteen ninety nine [promotional pamphlet], p. 11. See also www.bontrager.com.
4. Ritchey web site: http://www.ritchey-logic.com/products/components/n_rims/home_rims.htm.

## REFERENCES

Brandt, Jobst. 1983. *The bicycle wheel*, rev. ed. Menlo Park, CA: Avocet, p. 131. A book no wheelbuilder's library is complete without.

Forbes, V. 1998–99. Predicting wheel strength from hubs. *Human Power.* 46:8–10.

Schraner, G. 1999. *The art of wheelbuilding.* Denver: Buopane Publications, p. 44. Recent publication from DT with many insider tips from the European professional racing circuit.

Sutherland, H. 1995. *Sutherland's handbook for bicycle mechanics*, 6th ed. Berkeley: Sutherland Publications, pp. 11–25 *ff.*

**ACKNOWLEDGMENTS**

The author thanks David Gordon Wilson for his invaluable comments during the preparation of this article, Helios Studios in Columbia, MO, John W. Stephens of Garden Grove, CA, and Jean Seay of San Luis Obispo, CA, for their assistance in the preparation of this article.

Figure 1 is after *The Bicycle Wheel* by Jobst Brandt and appears by his courtesy and with his permission. The author thanks him for his comments in reading an advance copy of this article.

Figure 2 is after the Bontrager Components homepage, http://www.bontrager.com, and appears courtesy of Keith Bontrager and with his permission.

The author thanks Tryathletics in Columbia, Missouri, without whom this article would not be possible.

---

*Vernon is a bike mechanic in Columbia, Missouri. Requests for reprints should be sent with a with a self-addressed envelope and sufficient postage (two international postal reply coupons for outside the USA) to him at:*

*—Vernon Forbes*
*1007 Grand Ave*
*Columbia, MO 65203-4025 USA*
*Telephone: 573-442-0687*
*vforbes@coin.org*

## UPDATE

**From Anil Rajvanshi, author of Cycle Rickshaws, HP 49 (Winter 1999–2000)**

I liked your comment on poor quality of present cycles and am trying to make rickshaws keeping this point of view very much in mind. The consumer movement is catching up in India and a couple of two-wheeler manufacturers have been taken to court for poor manufacturing. I hope the same could be done for cycles and rickshaws.

We are now putting twenty MAPRs in Lucknow and will be very interested in sharing our experiences with your readers. I plan to visit the US this summer and would like to meet interested people.

*With warm regards,*
*—Anil Rajvanshi*
*anilrajvanshi@vsnl.com*

# Rolling resistance of bicycle tyres

***by John Lafford***

## INTRODUCTION

I have been a research and development engineer for many years, and when I started recumbent racing about fourteen years ago, it was only natural for me to want to obtain reliable data on cycling performance. The most important factor is aerodynamics, and I addressed the measurement of aerodynamic drag in the real world by doing coast-down tests. The procedure for this is described in “So you want to build an HPV”, (p. 40 *ff*) a publication of the British Human Power Club. For an accurate drag result you also need to know the rolling-resistance values for the tyres. As you go faster, the rolling resistance becomes more important and it is therefore vital to have accurate data on which to base a tyre choice. It was this requirement that led to study and analysis to derive an accurate and repeatable test procedure for measuring rolling resistance.

The testing has all been done with racing in mind. For touring or commuting other factors such as wear resistance, puncture resistance, grip in the dry and wet, and cost, come into consideration for tyre choice.

## TESTING PROCEDURE

The tyre-testing procedure involves rolling the tyre/wheel combination along a flat surface and so represents the real case of using the tyre on the road. The tyre is also loaded with a representative weight and starts rolling at a controlled initial speed. The distance that the tyre rolls is inversely proportional to the rolling resistance. The rolling-resistance coefficient is derived from knowing the initial speed and the distance that the tyre rolls.

The speed of rolling in the tests is slow so that aerodynamic forces are negligible. The flat surface used is fairly smooth concrete in my local aircraft-factory workshop, and is reasonably representative of a smooth tarmac road surface. In any event, as all the tests are performed in exactly the same place, they all relate to one another.

The power to propel tyres along the road (Prr), is directly proportional to the rolling-resistance coefficient (Crr), the weight of the vehicle plus rider (W), and also the speed of the vehicle (V).

Prr = Crr x W × V (times a constant for users of ancient units –*ed.*)

The power absorbed is the same whether the vehicle has two, three or four wheels (so long as they are perfectly aligned, as the author confirms below –*ed.*). In the table, the power is computed in watts for the cases of (1) vehicle plus rider weighing 185 lb (84 kg) at road speeds of 20 mph, 25 mph and 30 mph (32 kph, 40 kph and 48 kph, respectively); and (2) vehicle plus rider weighing 200 lb (91kg) at road speeds of 30 mph, 40 mph and 50 mph (48 kph, 64 kph and 80 kph, respectively) which is relevant to faired vehicles.

## TIME LOST

The time-lost column gives a practical appreciation of the importance of the rolling resistance of the tyre by showing the time lost by each of the tyres against the best tyre listed (the last tyre in the list), over a distance of 10 miles (16 km). The base time for 10 miles at 25 mph is 24.00 minutes.

The time lost is derived from aerodynamic-drag values obtained in coast-down test results (see reference below) using my own racing recumbent. Data from the test will predict the power required to ride along a level road at 25 mph and 24 mph. The difference in these two values was 28 watts for my recumbent with the average tyres that were fitted at that time. The time taken to ride 10 miles at 24 mph is 25.00 minutes. The time-lost column is calculated by proportion of the power absorbed by each of the tyres compared to the Vredestein Fortezza Piste:

Time lost for tyre ‘a’ = [Prr(tyre ‘a’) –Prr(Vredestein)] x 60/28

It can be seen that using the wrong tyres can easily cause one to lose over a minute over the 10 miles.



## COMMENTARY ON THE TABLE

1. Some of the tyres are tested at pressures above the manufacturer,s recommended pressure. This was done for scientific interest. This does not imply approval of operating tyres above the manufacturer,s recommended pressure.
2. Most of the tyres are tested at several pressures to show the effect of pressure on rolling performance.
3. The list includes the effect of grinding the tread down on some tyre types. This simulates the effect of tyre wear. This generally gives an improvement in rolling performance. In some cases it is not beneficial as the tyre sidewall flexibility may be a more important factor in absorbing energy as the tyre rolls.
4. The list includes some examples of the effect of using latex inner tubes instead of butyl inner tubes. Generally, the latex tube will give an improvement. However, if the tyre has a thick tread, this will dominate the energy absorption, and latex will show no benefit. Latex gives a good improvement where the tyre tread is thin and flexible so that the reduction in energy caused by substituting the butyl tube can be seen.
5. The 700c tyres shown are among the very best on the market. Most 700c tyres are not nearly as good as these. Some 700c tyres are very poor. Do not be misled into thinking all 700c tyres are good just because the three shown are good.
6. General rules for good rolling performance:
   a. thin-tread-thickness tyres roll better;
   b. fat-section tyres roll better;
   c. knobbly tyres roll badly;
   d. Kevlar™ often gives poor rolling performance (except Vittoria); and
   e. used tyres roll better than new tyres as they are thinner, and therefore more flexible.
7. One cannot assume that all tyres from a particular manufacturer are fast or slow. Generally they have a range of rolling performance that does not necessarily have any relationship with the company’s advertising claims.
8. For additional rolling-resistance data, see reports in the following British magazines:
*Cycling Plus*, issue 62 (Feb. ’97) “Winter tyres”; *Cycling Plus*, issue 68 (Mid-summer ’97) “Road tyres”; *Cycling Plus*, issue 81 (Aug ’98) “Time-trial tyres”; *Total Bike*, issue 6 (Oct ’97) “MTB tyres”; and *BHPC Newsletter*, issue 58, “MTB tyres”.
9. Thanks are due to the following for the loan of tyres for testing: Hilary Stone, Richard Grigsby, John Kingsbury, Michelin Tyres, Cambrian Tyres, Dillglove (Nokian tyres).

---

*John Lafford <jalafford@aol.com>*
*John Lafford is an engineer who has been building and racing recumbents for 14 years. He is interested in all the technical aspects of cycling with emphasis on efficiency of operation. He has built two- and three-wheeled recumbents, both faired and unfaired, and also works on power-assisted bikes and trikes. He also takes part in time-trial events using a cross-shaped-frame design of bicycle produced by his own Arrow Bicycle Company.*

---

(Editor’s note: discussion of contributions is always welcome in letters to *Human Power*. John Lafford’s contribution included values that varied from those of others, and I asked Jim Papadopoulos to comment. Then I sent his comments to John for a response. I would like to thank both for their courtesy in discussing the results and in allowing us to publish their remarks.

*—Dave Wilson)*

### Note on Lafford’s paper and spreadsheet

by Jim Papadopoulos

It is always heartening to see evidence of a great deal of careful testing. I appreciate that Lafford actually did something, rather than just talk about it (as I am prone to do). Of course his numbers raise a host of questions. None of these are criticisms per se, but the answers might help establish how reliable his results really are.

I did not grasp immediately that his focus was primarily on small wheels. Spreadsheet and article should perhaps be called “Rolling resistance of small-diameter tires”.

My questions relate primarily to accuracy and meaningful precision of his data.

How repeatable is his test? The fact that an increasing series of inflation pressures leads to a decreasing series of rolling resistance coefficients suggests that his final digit is meaningful (+0.0001). However it would be good to have a statement from John about how well his tests repeat, what averaging he employs, etc. How accurate is his test? Here my questions spring from a couple of disparate perspectives.

1. How do his numbers compare with others’? He gives “good 700C” numbers of 0.0043–0.0046; however some other sources give numbers 0.0019–0.0033.

His best Moulton number is 0.0079 whereas Kyle has given 0.0030 and Burke gave 0.0038. I would feel better if Lafford had been able to duplicate some other accepted result.

2. Has he taken care to eliminate some of the “obvious” errors one expects in this kind of low-speed, “coasting to rest” test? Low-speed rolling is strongly affected by minor (invisible) slopes. (In the hallway at Cornell, for example, there was an invisible dip that would clearly accelerate a rider.) His results lose force if either (a) the paths differ from time to time or (b) in going down and up, some wheels “stall” while others just manage to “crest” a rise and travel much further. Also, I wonder how the wheel is balanced and guided as it comes to rest. The normal way is to make a tricycle, but then there is an issue of drag from the support wheels (particularly if their alignment is faulty). That support drag could perhaps be subtracted, but only if it was known with high accuracy. In my own researches I had hoped to try castering one of the two lightly loaded support wheels, but never got around to it. Finally some comments about conditions:

• Because the measurement was taken at low speed, then the high-speed calculations should have a disclaimer. Kyle believes there is a speed effect, for example.

***Turn to page 18***

# Rolling resistance of tyres - test data

***© John Lafford, Nov 1999***

Generally available recumbent tyres
(Butyl inner tubes unless stated)

Rolling resistance power absorbed
Unfaired wgt = 185 lb/84 kg / Faired wgt = 200 Lb/91 kg

| Tyre name | Size | Test pressure psi* | Rolling res coef. Crr test | Prr 20mph 32kmh† watts | Prr 25mph 40kph watts | Prr 30mph 48kph watts | Prr 30mph 48kph watts | Prr 40mph 64kph watts | Prr 50mph 80kph watts | Time lost @ 25mph over 10 mi.† sec. |
|---|---|---|---|---|---|---|---|---|---|---|
| IRC Road Lite (new) | 20" x 1 1/8" | 100 | 0.0090 | 66 | 82 | 99 | 107 | 143 | 178 | 92 |
| IRC Road Lite (new) | 20" x 1 1/8" | 115 | 0.0089 | 65 | 82 | 98 | 106 | 141 | 176 | 90 |
| Conti Top Touring (new) | 37-406 | 70 | 0.0092 | 68 | 84 | 101 | 110 | 146 | 183 | 96 |
| Conti Top Touring (new) | 37-406 | 90 | 0.0079 | 58 | 73 | 87 | 94 | 126 | 157 | 71 |
| IRC Road Lite (old) | 20" x 1 1/8" | 100 | 0.0068 | 50 | 63 | 75 | 81 | 108 | 136 | 49 |
| IRC Road Lite (old) | 20" x 1 1/8" | 115 | 0.0064 | 47 | 59 | 71 | 77 | 102 | 128 | 41 |
| Michelin | 28-440 | 70 | 0.0078 | 57 | 71 | 86 | 93 | 123 | 154 | 68 |
| Michelin | 28-440 | 90 | 0.0071 | 52 | 65 | 78 | 84 | 112 | 141 | 54 |
| Tioga Comp Ramp (new) | 20 x 1 7/8 | 85 | 0.0080 | 59 | 73 | 88 | 95 | 127 | 159 | 72 |
| Tioga Comp Ramp (new) | 20 x 1 7/8 | 100 | 0.0079 | 58 | 73 | 87 | 95 | 126 | 158 | 71 |
| Hutchinson HP 25 | 25-451 | 115 | 0.0080 | 59 | 74 | 88 | 95 | 127 | 159 | 73 |
| Hutchinson HP 25 | 25-451 | 90 | 0.0089 | 65 | 81 | 98 | 106 | 141 | 176 | 89 |
| Hutchinson HP 25 | 25-451 | 100 | 0.0086 | 63 | 79 | 95 | 103 | 137 | 171 | 84 |
| Conti Top Touring (new) | 37-406 | 70 | 0.0090 | 66 | 83 | 99 | 108 | 143 | 179 | 93 |
| Conti Top Touring (new) | 37-406 | 90 | 0.0081 | 60 | 74 | 89 | 97 | 129 | 161 | 74 |
| Conti Top Touring (new) | 37-406 | 100 | 0.0080 | 59 | 74 | 89 | 96 | 128 | 160 | 73 |
| Conti Top Touring (new) | 37-406 | 115 | 0.0084 | 62 | 77 | 93 | 100 | 133 | 167 | 80 |
| Michelin (450 x 28A) | 28-390 | 100 | 0.0065 | 48 | 60 | 72 | 78 | 104 | 130 | 43 |
| Michelin (450 x 28A) | 28-390 | 115 | 0.0064 | 47 | 59 | 71 | 77 | 102 | 128 | 42 |
| Conti Grand Prix (new) | 28-406 | 100 | 0.0072 | 53 | 67 | 80 | 86 | 115 | 144 | 57 |
| Conti Grand Prix (new) | 28-406 | 120 | 0.0067 | 49 | 61 | 74 | 80 | 106 | 133 | 47 |
| Conti Grand Prix (new) | 28-406 | 140 | 0.0066 | 49 | 61 | 73 | 79 | 105 | 132 | 45 |
| Vee Rubber (new) | 20 x 2.125 | 40 | 0.0114 | 84 | 105 | 126 | 136 | 181 | 226 | 139 |
| Vee Rubber (new) | 20 x 2.125 | 60 | 0.0105 | 77 | 96 | 116 | 125 | 167 | 209 | 122 |
| Vee Rubber (new) | 20 x 2.125 | 80 | 0.0097 | 72 | 89 | 107 | 116 | 155 | 193 | 107 |
| Primo 16 x 1 3/8 (new) | 37-349 | 100 | 0.0078 | 57 | 72 | 86 | 93 | 124 | 155 | 69 |
| Primo 16 x 1 3/8 (new) | 37-349 | 110 | 0.0071 | 52 | 65 | 78 | 85 | 113 | 141 | 55 |
| Primo 16 x 1 3/8 (new) | 37-349 | 120 | 0.0070 | 52 | 65 | 78 | 84 | 112 | 140 | 54 |
| Tioga Comp Pool (new) | 20 x 1.75 | 90 | 0.0074 | 54 | 68 | 81 | 88 | 117 | 146 | 60 |
| Tioga Comp Pool (new) | 20 x 1.75 | 100 | 0.0071 | 52 | 65 | 78 | 84 | 113 | 141 | 54 |
| Tioga Comp Pool (new) | 20 x 1.75 | 110 | 0.0069 | 51 | 63 | 76 | 82 | 110 | 137 | 51 |
| Tioga Comp Pool (new) | 20 x 1.75 | 120 | 0.0065 | 48 | 60 | 72 | 78 | 103 | 129 | 43 |
| Kenda w. tread ground off | 16 x 1.75 | 80 | 0.0068 | 50 | 63 | 76 | 82 | 109 | 136 | 50 |
| Kenda w. tread ground off | 16 x 1.75 | 90 | 0.0064 | 47 | 59 | 70 | 76 | 101 | 127 | 41 |
| Kenda w. tread ground off | 16 x 1.75 | 100 | 0.0066 | 48 | 60 | 72 | 78 | 104 | 130 | 44 |
| Michelin Hilite S'compHD | 650 x 20c | 100 | 0.0062 | 45 | 57 | 68 | 74 | 98 | 123 | 36 |
| Michelin Hilite S'compHD | 650 x 20c | 110 | 0.0058 | 43 | 53 | 64 | 69 | 92 | 115 | 29 |
| Michelin Hilite S'compHD | 650 x 20c | 120 | 0.0055 | 40 | 50 | 60 | 65 | 87 | 109 | 22 |
| Hutchinson HP 25 | "600A x 24""" | 100 | 0.0070 | 52 | 65 | 77 | 84 | 112 | 140 | 53 |
| Hutchinson HP 25 | "600A x 24""" | 120 | 0.0068 | 50 | 63 | 76 | 82 | 109 | 136 | 50 |
| Hutchinson HP 25 | "600A x 24""" | 140 | 0.0068 | 50 | 63 | 75 | 81 | 109 | 136 | 50 |
| Primo V Monster (new) | 20 x 1.75 | 65 | 0.0074 | 55 | 68 | 82 | 89 | 118 | 148 | 61 |
| Primo V Monster (new) | 20 x 1.75 | 80 | 0.0078 | 57 | 72 | 86 | 93 | 124 | 155 | 68 |
| Michelin | 600 x 28A | 80 | 0.0075 | 55 | 69 | 83 | 89 | 119 | 149 | 62 |
| Michelin | 600 x 28A | 100 | 0.0072 | 53 | 66 | 79 | 86 | 115 | 143 | 57 |
| Primo w/ground off tread | 37-349 | 85 | 0.0066 | 49 | 61 | 73 | 79 | 106 | 132 | 46 |
| Primo w/ground off tread | 37-349 | 100 | 0.0063 | 47 | 58 | 70 | 76 | 101 | 126 | 40 |
| Primo w/ground off tread | 37-349 | 110 | 0.0064 | 47 | 59 | 70 | 76 | 102 | 127 | 41 |
| Primo w/ground off tread | 37-349 | 120 | 0.0060 | 44 | 55 | 66 | 71 | 95 | 119 | 33 |
| Primo w/ground off tread | 37-349 | 140 | 0.0060 | 44 | 55 | 66 | 71 | 95 | 119 | 33 |
| Moulton Wolber line tread (new) | 17 x 1 1/8 | 70 | 0.0092 | 68 | 85 | 102 | 110 | 147 | 184 | 97 |
| Moulton Wolber line tread (new) | 17 x 1 1/8 | 100 | 0.0084 | 62 | 78 | 93 | 101 | 134 | 168 | 81 |
| Moulton Wolber line tread (new) | 17 x 1 1/8 | 120 | 0.0079 | 58 | 73 | 87 | 94 | 126 | 157 | 71 |
| Primo w/ground off tread, latex tube | 37-349 | 100 | 0.0066 | 49 | 61 | 73 | 79 | 106 | 132 | 46 |

* 1 bar = 14.5 psi; † 1 m/s = 3.6 kmh;
† compared with the time using the tyre (at the same power input) with lowest Crr, the last entry in the table



Rolling resistance power absorbed
Unfaired wgt = 185 lb/84 kg / Faired wgt = 200 Lb/91 kg

| Tyre name | Size | Test pressure psi* | Rolling res coef. Crr test | Prr 20mph 32kmh† watts | Prr 25mph 40kph watts | Prr 30mph 48kph watts | Prr 30mph 48kph watts | Prr 40mph 64kph watts | Prr 50mph 80kph watts | Time lost @ 25mph over 10 mi.† sec. |
|---|---|---|---|---|---|---|---|---|---|---|
| Primo w/ground off tread, latex tube | 37-349 | 120 | 0.0061 | 45 | 56 | 67 | 73 | 97 | 121 | 35 |
| Primo w/ground off tread, latex tube | 37-349 | 140 | 0.0058 | 42 | 53 | 64 | 69 | 92 | 115 | 29 |
| Vredestein Monte Carlo (new) | 37-406 | 90 | 0.0069 | 51 | 63 | 76 | 82 | 109 | 137 | 50 |
| Vredestein Monte Carlo (new) | 37-406 | 100 | 0.0067 | 49 | 62 | 74 | 80 | 107 | 134 | 47 |
| Vredestein Monte Carlo (new) | 37-406 | 120 | 0.0064 | 47 | 58 | 70 | 76 | 101 | 126 | 40 |
| Hutchinson | 600 x 28A | 100 | 0.0059 | 43 | 54 | 65 | 70 | 94 | 117 | 31 |
| Hutchinson | 600 x 28A | 120 | 0.0052 | 38 | 48 | 58 | 62 | 83 | 104 | 18 |
| Conti Grand Prix w/latex tube | 28-406 | 100 | 0.0077 | 57 | 71 | 85 | 92 | 123 | 153 | 67 |
| Conti Grand Prix w/latex tube | 28-406 | 125 | 0.0069 | 51 | 64 | 77 | 83 | 110 | 138 | 52 |
| Conti Grand Prix w/latex tube | 28-406 | 140 | 0.0067 | 49 | 61 | 74 | 80 | 106 | 133 | 47 |
| Schwalbe Spezial City Jet (used) | 32-406 | 100 | 0.0065 | 48 | 60 | 72 | 78 | 104 | 130 | 44 |
| Schwalbe Spezial City Jet (used) | 32-406 | 120 | 0.0063 | 46 | 58 | 70 | 75 | 100 | 126 | 39 |
| Nokian City Runner (new) | 40-406 | 72 | 0.0083 | 61 | 76 | 91 | 99 | 131 | 164 | 78 |
| Nokian City Runner (new) | 40-406 | 100 | 0.0078 | 58 | 72 | 86 | 93 | 124 | 156 | 69 |
| Nokian City Runner (new) | 40-406 | 120 | 0.0071 | 52 | 65 | 78 | 85 | 113 | 141 | 55 |
| Nokian Mount & City (new) | 47-406 | 50 | 0.0083 | 61 | 76 | 91 | 99 | 132 | 165 | 78 |
| Nokian Mount & City (new) | 47-406 | 80 | 0.0072 | 53 | 66 | 79 | 86 | 114 | 143 | 57 |
| Nokian Mount & City (new) | 47-406 | 100 | 0.0068 | 50 | 63 | 75 | 81 | 109 | 136 | 49 |
| Nokian Mount & City (new) | 47-406 | 120 | 0.0063 | 47 | 58 | 70 | 76 | 101 | 126 | 40 |
| Nokian Mount & Ground (used) | 47-406 | 45 | 0.0104 | 76 | 95 | 114 | 124 | 165 | 206 | 119 |
| Nokian Mount & Ground (used) | 47-406 | 80 | 0.0100 | 73 | 92 | 110 | 119 | 159 | 198 | 112 |
| Nokian Mount & Ground (used) | 47-406 | 100 | 0.0089 | 66 | 82 | 99 | 107 | 142 | 178 | 91 |
| Schwalbe City Jet (new) | 32-406 | 100 | 0.0087 | 64 | 80 | 96 | 104 | 139 | 174 | 87 |
| Schwalbe City Jet (new) | 32-406 | 120 | 0.0082 | 60 | 76 | 91 | 98 | 131 | 163 | 77 |
| Schwalbe Marathon (new) | 32-406 | 100 | 0.0097 | 72 | 89 | 107 | 116 | 155 | 193 | 107 |
| Schwalbe Marathon (new) | 32-406 | 115 | 0.0101 | 75 | 93 | 112 | 121 | 161 | 201 | 114 |
| Schwalbe Marathon (new) | 32-406 | 130 | 0.0100 | 73 | 92 | 110 | 119 | 159 | 198 | 112 |
| Vredestein Monte Carlo (used) | 37-406 | 90 | 0.0077 | 57 | 71 | 85 | 92 | 123 | 154 | 67 |
| Vredestein Monte Carlo (used) | 37-406 | 100 | 0.0069 | 51 | 64 | 76 | 82 | 110 | 138 | 51 |
| Vredestein Monte Carlo (used) | 37-406 | 120 | 0.0068 | 50 | 63 | 75 | 81 | 109 | 136 | 50 |
| Nokian Mount & City (new) | 47-305 | 50 | 0.0135 | 100 | 124 | 149 | 161 | 215 | 269 | 182 |
| Nokian Mount & City (new) | 47-305 | 80 | 0.0103 | 76 | 95 | 114 | 123 | 164 | 205 | 118 |
| Primo 20 x 1.5 (used) | 37-451 | 85 | 0.0066 | 48 | 61 | 73 | 79 | 105 | 131 | 45 |
| Primo 20 x 1.5 (used) | 37-451 | 100 | 0.0065 | 48 | 60 | 71 | 77 | 103 | 129 | 43 |
| Primo 20 x 1.5 (used) | 37-451 | 120 | 0.0062 | 46 | 57 | 69 | 75 | 99 | 124 | 38 |
| IRC Roadlite 20 x 1 1/8 (used) | 28-451 | 100 | 0.0068 | 50 | 63 | 76 | 82 | 109 | 136 | 50 |
| IRC Roadlite 20 x 1 1/8 (used) | 28-451 | 120 | 0.0064 | 47 | 59 | 71 | 77 | 102 | 128 | 42 |
| Primo Comet | 37-406 | 100 | 0.0074 | 54 | 68 | 82 | 88 | 118 | 147 | 61 |
| Primo Comet | 37-406 | 120 | 0.0070 | 52 | 64 | 77 | 84 | 111 | 139 | 53 |
| Michelin (used) | 600 x 28A | 70 | 0.0081 | 59 | 74 | 89 | 96 | 128 | 160 | 74 |
| Michelin (used) | 600 x 28A | 90 | 0.0073 | 54 | 68 | 81 | 88 | 117 | 146 | 60 |
| Continental Grand Prix (used) | 28-406 | 120 | 0.0082 | 60 | 76 | 91 | 98 | 131 | 163 | 77 |
| Haro (used) | 20 x 1.5 | 65 | 0.0073 | 54 | 68 | 81 | 88 | 117 | 146 | 60 |
| Haro (used) | 20 x 1.5 | 85 | 0.0068 | 50 | 63 | 75 | 81 | 108 | 136 | 49 |
| Haro (used) | 20 x 1.5 | 100 | 0.0063 | 47 | 58 | 70 | 76 | 101 | 126 | 40 |
| Haro (new) | 20 x 1.5 | 65 | 0.0077 | 56 | 70 | 84 | 91 | 122 | 152 | 66 |
| Haro (new) | 20 x 1.5 | 85 | 0.0067 | 50 | 62 | 74 | 80 | 107 | 134 | 48 |
| Nokia Mount and City (new) | 47-406 | 50 | 0.0104 | 77 | 96 | 115 | 124 | 165 | 207 | 120 |
| Nokia Mount and City (new) | 47-406 | 70 | 0.0087 | 64 | 80 | 96 | 104 | 139 | 174 | 87 |
| Nokia Mount and City (new) | 47-406 | 90 | 0.0082 | 60 | 75 | 90 | 98 | 130 | 163 | 76 |
| Nokia Mount and City (new) | 47-406 | 100 | 0.0073 | 54 | 67 | 81 | 87 | 116 | 145 | 59 |
| Vredestein S-Lick (new) | 32-406 | 60 | 0.0155 | 114 | 142 | 171 | 185 | 246 | 308 | 220 |
| Vredestein S-Lick (new) | 32-406 | 90 | 0.0106 | 78 | 97 | 117 | 126 | 168 | 210 | 123 |
| Vredestein S-Lick (new) | 32-406 | 100 | 0.0098 | 72 | 90 | 108 | 117 | 155 | 194 | 107 |
| RECOMMENDED 700C TYRES FOR REAR WHEELS for comparison. Very good performance at reasonable price. | | | | | | | | | | |
| Nokia Roadie (used) | 700 x 25c | 100 | 0.0046 | 34 | 42 | 51 | 55 | 73 | 91 | 5 |
| Michelin Axial Supercomp | 23-622 | 110 | 0.0046 | 34 | 42 | 51 | 55 | 73 | 91 | 5 |
| Vredestein Fortezza Piste | 700 x 23c | 10 bar | 0.0043 | 32 | 40 | 48 | 52 | 69 | 86 | 0 |

* 1 bar = 14.5 psi; † 1 m/s = 3.6 kmh;
† compared with the time using the tyre (at the same power input) with lowest Crr, the last entry in the table

• What was his load? “Representative” probably means it was 45 kg, but it would be nice to know for sure.

None of this is meant as direct criticism of Lafford’s careful efforts, but rather as an invitation to discuss some vitally interesting issues!

*—Jim Papadopoulos*

**Reply to note by Jim Papadopoulos, approximately in the order of his questions,**

***Tires tested.*** The number of tyres tested is approaching 400 and I have tested tyres of all sizes. The article was focused on small-diameter tyres as they are of particular interest to HPV riders. I included three good 700C tyres of good value.

***Repeatability***

1. If I run a tyre up the track and it runs 20' 3" (say), and then I repeat it straight away and follow the exact same piece of the floor, then it also will run 20' 3". If the direction is a bit off then the distance will be slightly different due to the slight imperfections in the floor.

2. If I were to repeat the test on that tyre on another day, then I might not have exactly the same pressure in the tyre by 1 or 2 psi, and the temperature would probably be different and so there would be a slightly different result. I have a simple test for this type of repeatability, where I have a particular Michelin tyre which I run from time to time. This has shown over a period of 18 months and 7 test sessions that the Crr value is repeatable at 0.0051 to ± 0.0001 and the power absorbed at 25 mile/h to be 47 watts to ± one watt. I have always rounded the power-absorbed figure off to a whole number as it would be unreasonable to assume better accuracy than this.

***Averaging***

Jim Papadopoulos clearly appreciates some of the practical problems in running the tests. Yes, the floor does have very slight undulations in it. To cater for this, in the area available, I ran the tyre-test rig backwards and forwards in many directions to find a line that gave the same rolling distance, running in both directions. Then, to cope with the very slight undulations in the floor, the floor is marked out at 4' intervals from the start point of the test run. A stop watch is used and the time recorded for the test rig to pass the 4', 8', 12', 16', 20', 24', 28', etc. markers. In the coast-down test, the retardation should be completely uniform, and so several of the 4' zones are averaged to give a mean average retardation. This avoids any errors caused by cresting or failing to crest a slight rise at the end of a test run.

***Comparing my data with other sources***

There are some better 700C than those I listed, but I did not include these as they are more expensive and less durable. There are many 700c tyres a whole lot worse.

The Moulton data are for the line tread, touring tyre, not the high-pressure slick.

I am not looking to repeat other people’s results. It would be relevant only if I had the same tyres that they had used.

The test wheel/tyre is fitted to a tricycle. The two other wheels are perfectly aligned, I know their rolling-resistance coefficient and they are only lightly loaded. Even so, their rolling coefficient and load and drag components are taken into account.

The weight on the test wheel is 66 lb. This is representative for three wheelers, which many HPVs are, but is light for a two-wheeler. It is chosen for convenience of installation and the number of times I have to pick it up and load it onto the trike test rig. Further, I have tested with a heavier weight and got a very similar result. As long as all my tests are done under the same conditions then the results are properly comparative. Most of the applied weight is directly on the test wheel. It cannot be exactly on it because the tricycle would not then be stable. However, as the position is known, moments are taken, and the exact weight used in the computations.

*—John Lafford*

## TECHNICAL NOTES

### Power requirements for laid-back recumbents

*Report and comment by Dave Wilson, with translation help from Jan Limburg and Ellen Wilson.*

This is an interpretation of the high points of an article by Bert Hoge and Jeroen Schasfoort in HPV nieuws no. 4, 1999, the magazine of the Netherlands NVHPV. Its topic is the use of an SRM instrumented crank (giving torque) on a “regular” racing bike and on five recumbents. All of the recumbents were of the very-laid-back variety, having seat-back angles with the horizontal of down to 15 degrees (see photos). All of them had the bottom-bracket considerably above the lowest part of the seat: I believe that this is important because whirling legs normally give a high drag, and having them in the “forward shadow” of the body must reduce this drag. The authors write, “A smaller frontal surface gives less air resistance and higher speed. It can be achieved by increasing the height of the bottom bracket above the lowest part of the seat to about 270 mm (10.6"), and reducing the seat height to about 250 mm (9.8").” (These are approximately the relevant measurements of the M5 Low Racer.) All six bicycles were ridden by one tester, Dries Baron, weight 90 kg (198 lb.), height 1.86 m. (6'1", almost a midget by Dutch standards) wearing racing clothing, on a 200-m-long velodrome track, presumably oval or circular. Ten circuits (2 km total) were made for each test point. All bicycles used Continental Grand-Prix or IRC tires pumped to about 8-bar pressure (116 psi). Two speeds were chosen: 30 and 40 kmh (18 and 25 mph), and the cadence was kept to about 88 rpm. The temperature was about 15 C, 59 F. The measurement accuracy was reckoned to be ±2% (see graph, figure 1).

The racing or “road” bike was ridden in the “touring” position, which I believe meant that the hands were on top of the handlebars, rather than the rider being in a full crouch. All of the recumbents required less power to propel them than did the “regular” racing bike in this configuration. The reduction appeared to be a function of how low the rider was (see photos). The lowest power of the unfaired recumbents was needed by Bram Moens’ M5, which at 40 kmh took 228 W, while the racing bicycle required 389 W input. The fully-faired M5 required less than 130 W at the same speed. (Table 1)

These results can be compared with the aerodynamic drag measured in the “Tour” tests of stationary bikes in the wind-tunnel and on bikes being ridden on a velodrome, reviewed in *Human Power*, 12:4, spring 1997. There is general qualitative agreement, although only the faired M5 and the regular bikes were common to both tests. The LWB “Peer Gynt” with low bottom-bracket was found to have a higher drag than that of a regular racing bike with the rider in a full crouch. Because of the difference in the rider positions on the racing bike, the principal interest in the results shown here is in the differences among the recumbents, and in the accuracy of actual power measurements taken on different bicycles with the same rider on the same circuit with similar tires.

These are very valuable data. Thank you, Bert Hoge, Jeroen Schasfoort and the NVHPV!

*—Dave Wilson*

**Table 1: Power required to propel bicycles**

| Bicycle type or name | Power, watts 30 kmh | Power, watts 40 kmh | Expected increase in speed* |
|---|---|---|---|
| Racing bike, touring position | 181 | 389 | 0% |
| Optima Dolphin | 161 | 336 | 6% |
| Flevobike 50-50 | 152 | 309 | 10% |
| M5 20-20 | 131 | 265 | 17% |
| Baron Low Racer | 128 | 251 | 20% |
| Moens (M5) Low Racer | 114 | 228 | 24% |

*Relative to racing bike

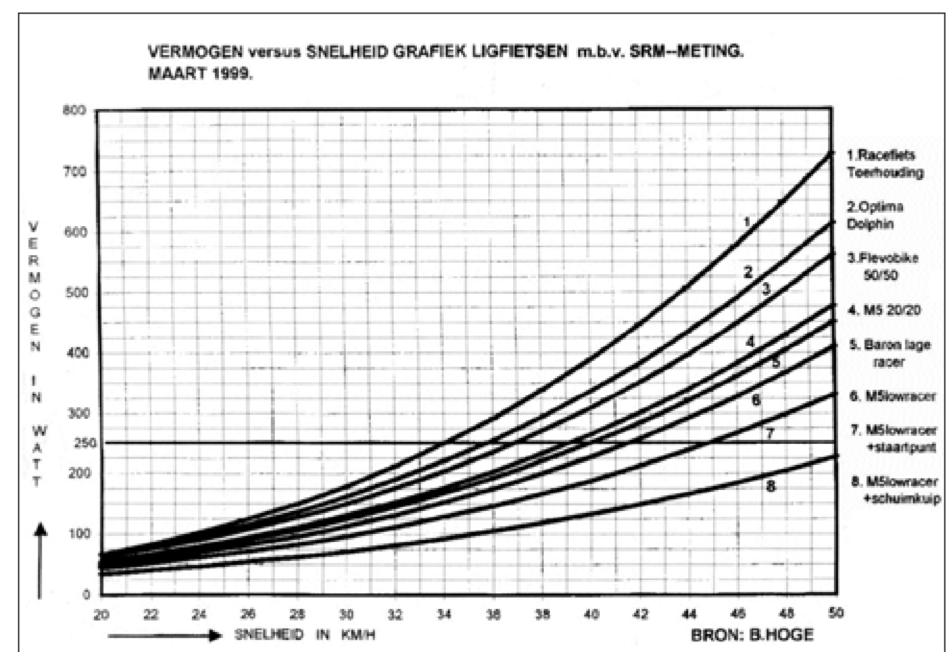


**Figure 1. Power (watts) required vs. speed (kph).**

**Figure2. Bicycles tested.**

**Optima Dolphin**

**Flevobike Fifty Fifty**

**M5 20 20**

**Baron low racer**

**M5 low racer**

—Photos and chart courtesy *HPV nieuws;* prepared for *Human Power* by JW Stephens

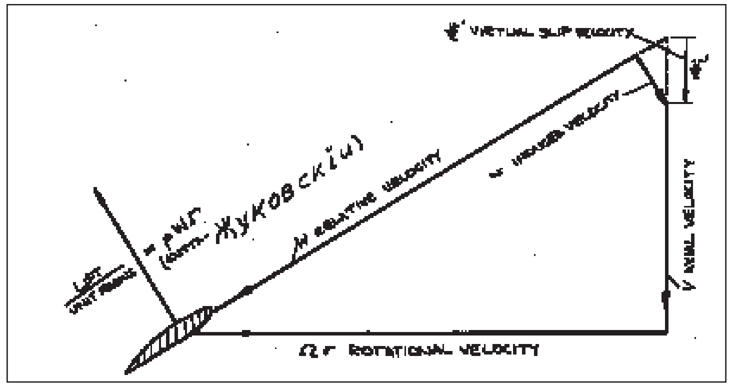


Figure 1. Blade-element velocities

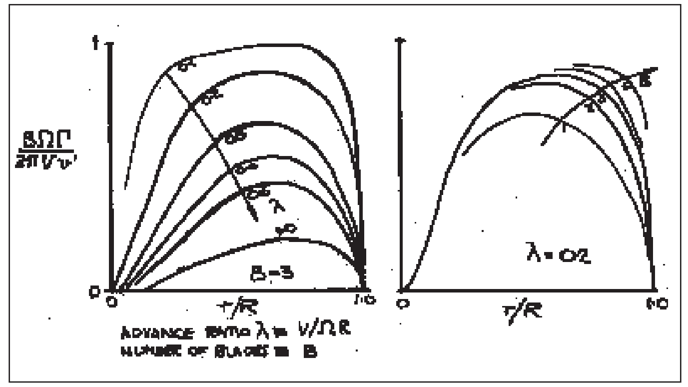


Figure 2. Blade radial-lift distributions

# My propeller theory

*by E. Eugene Larrabee*

In 1978 I developed a useful form of propeller theory based on the work of Hermann Glauert (1926 and 1938) and Sidney Goldstein (1929). It was successfully applied to the propellers of the Chrysalis and Gossamer Albatross human-powered airplanes in 1979, and (in reverse) to windmills for US Windpower, Inc. in 1980.

It is related to lifting-line theory as developed by Ludwig Prandtl and his associates at Göttingen during World War I. In it an induced velocity is developed parallel to the blade lift direction and perpendicular to the relative velocity of the blade section with respect to the air mass as shown in figure 1. The flight (or axial) velocity, the rotational velocity, and the induced velocity combine to produce the resultant velocity. The induced velocity is caused by lift on each blade section due to bound circulation according to the Kutta-Joukowski Law.

Strangely enough, if the induced velocity is small enough compared to the axial velocity it can be shown that the induced loss of the propeller is minimized if the virtual slip velocity is radially constant, corresponding to a certain radial variation of the bound circulation. As Albert Betz, Prandtl's associate,wrote in 1923 (NACA TR 116), "The flow behind a propeller having the least loss of energy is as if the screw surfaces passed over by the propeller were solidified into a solid figure and this were displaced backward in the non-viscous fluid with a given small velocity." The small displacement velocity is exactly twice the virtual slip velocity.

I calculated the radial bound circulation distributions for minimum induced loss by a process suggested by Glauert in 1938. The distributions are functions of the advance ratio and the number of blades as shown in figure 2. They correspond to elliptic span loading for a wing.

Apparently these circulation distributions are slightly in error, as suggested by Goldstein in 1929 and by my former student, Mark Drela, in 1982. In any event they were good enough to form the basis of a Fortran code written by Hyong Bang in 1978 to define the blade chord and pitch angles for the Chrysalis and Gossamer Albatross airplanes so that they had not only minimum induced loss but also minimum profile drag by choice of blade section and lift coefficient at the design point. They "were propellers of highest efficiency" in Glauert's words.

At the relatively low advance ratios of these propellers they are characterized by narrow outer blade chords and wide inboard ones with strong twist, having almost true geometric pitch, as shown in figure 3.

The same is true of the US Windpower windmills generated by a later Fortran code HELICE, written by Susan Elso French at MIT. In the case of windmills the displacement velocity is against the wind direction and the more curved portions of the blades are downwind. They were intended to leave a minimum hole in the air for a given power output for the average wind speed of a "windfarm of many windmills."

Since then Prof. Mark Drela has developed his own XROTOR code which is a finite-element adaptation of Goldstein's 1929 paper. XROTOR was used to design propellers for the Monarch and Daedalus airplanes. French's HELICE code was rewritten in Pascal as ELICA by Robert S. Grimes in a form suitable for IBM PCs in 1982. Both Prof. Ernst Schoberl and I have used ELICA for many years personally. I published my algorithms in 1980.

I am told that AeroVironment uses a form of them to design propellers for their airplanes including the Pathfinder, which holds the altitude record for propeller-driven airplanes.

—*E. Eugene Larrabee,*
*professor emeritus, MIT*
*1800 Knoxville Avenue*
*Long Beach, CA 90815 USA*
*November 1999*

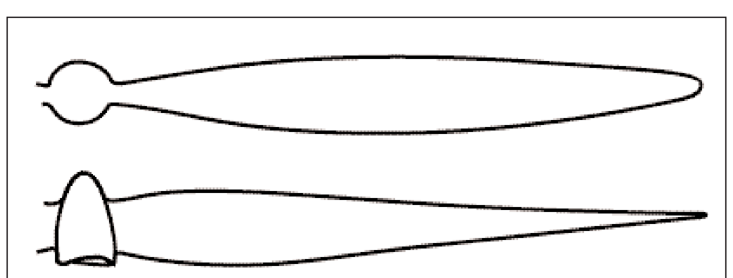

Figure 3. Shape of windmill blades produced by these methods.



## *REVIEWS*

### "Feet On!"
### a pedal-powered museum exhibit

***By Michael Eliasohn***

A bicycle is a relatively simple mechanism. A frame holds two wheels. A chain runs from the chain-ring to the sprocket attached to the rear wheel. Turn the pedals and the bike moves.

But how do you get those pedals to power a television or an organ, to light up light bulbs or create a vacuum, to blow 300 ping-pong balls around inside a chamber, or a moving sculpture, which consists of twelve bicycle wheels mounted on the wall?

That was the challenge facing Tom Caskey, science exhibit designer at the Southwestern Michigan (community) College Museum near Dowagiac, MI.

Caskey designed and, with some assistance, made the exhibits for the museum's "Feet On! The Power of Pedaling" exhibit, which ran from March 9 to June 12, 1999. He said he and other museum staff members came up with the idea for the exhibit.

Among the challenges in creating it was a budget of less than $1,000. So many of the pieces, such as bicycles and exercise bikes, were purchased at a Goodwill store (which sells second-hand goods) and at rummage sales. Some items were donated.

A lot of creativity was used. For instance, the organ parts were purchased at Goodwill, but the exhibit also used a metal trash can, garden hoses, a bellows from a previous museum exhibit and a bicycle pedal mechanism.

The squirrel-cage blower that moves the ping-pong balls around came from a furnace. "I had a blower...," Caskey said in explaining how he came up with the idea. "What are you going to do with a blast of air? I wanted something so that as people walked in the door, they could see a lot of action."

But the 300 ping-pong balls blown around in the clear plastic-walled chamber did more than move around. There were 294 white balls and six red ones. What were the odds of getting all the red ones to land in the six "pockets," which was half of an egg carton? "...about the same as winning the lottery," the accompanying sign stated.

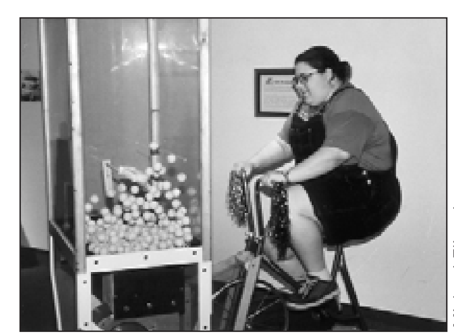

Michael Eliasohn

3) Marita English of Edwardsburg, MI, pedals the lottery exhibit. A squirrel-cage blower blows air into the chamber, to put 300 ping-pong balls into motion. "Winning" required putting the six red balls into the egg-carton pockets.

Caskey said he didn't expect anyone would beat the odds during the life of the exhibit, which taught visitors probability—and that it was unlikely they will ever win a lottery.

The device that shot a spark across a gap, to show that air is an insulator and the absence of air isn't, presented the opposite problem. Caskey adapted an old refrigerator compressor to act as a vacuum pump, to remove the air from inside a clear-plastic dome.

The television could be powered by one or two people sitting on a couch. The pedal mechanisms were two former exercise cycles, with the chains running to flywheels, and V-belts running from there to a generator.

To prevent one or two strong pedalers from "overpowering" the television, Caskey hooked up an electromagnetic brake designed for trailers, which acted on a disk on the generator shaft, making it impossible to "blow up" the television.

The other two pedal-powered exhibits were four light bulbs—the harder one pedaled, the more bulbs lit up—and a sculpture consisting of twelve bicycles wheels mounted on a wall, linked by ropes and chains, so that pedaling made the wheels rotate.

Caskey said a challenge in creating the pedal-powered exhibits was that they had to accommodate, in terms of muscles, everyone from little kids to football-player-sized men. "It's got to be responsive for both."

To accommodate various-sized riders, Caskey made super-long banana seats for some of the exhibits.

Michael Eliasohn

2) Leslie Gerschoffer (rear) and Marita English pedal what were exercise bikes, which power a generator which powers the television set they are watching. The TV could be "powered" by one or two people.

The mechanisms of the pedal-powered exhibits for the most part were exposed, so visitors could see how everything worked. "These are purposely made kid-understandable," said Caskey, whose museum job is part-time.

The "Feet On!" exhibit was located in the part of the SMC Museum, to paraphrase from its flier, devoted to hands-on science and technological exhibits that investigate scientific principles and the technological world that surrounds us.

The sign at the entrance read: "This exhibition is an exploration of energy transformation. The exhibits demonstrate how *your* energy is converted into other forms with interesting outcomes.

"You use chemical energy (namely food and drink) to feed your muscles—they are energy transformers. Your muscles allow you to move and give you the ability to move different things."

Making the exhibits pedal-powered was a means to make them "hands-on," or more correctly, "feet-on." "You're really involved," Caskey said.

The 59-year-old Caskey, whose background includes product and graphic design, making dulcimers and building a house, recently earned a master's degree in science education at Western Michigan University and wants to get a doctorate in the same topic.

The Feet On! exhibits illustrates Caskey's goal of making science learnable by being fun, not just by learning facts. "You can learn physics and subtlety and have fun ...," he suggested, "or you can think science is dumb stuff."

Michael Eliasohn

**4) Tom Caskey, designer/builder of the "Feet On! exhibit, pedals the exhibit that shot a spark across a gap inside a vacuum. The long banana seat enabled the exhibit to accommodate various-sized riders.**

*Tom Caskey can be contacted by e-mail at tcaskey@smc.cc.mi.us or by mail to Southwestern Michigan College Museum, 58900 Cherry Grove Road, Dowagiac MI 49047 • USA*

*Michael Eliasohn is a reporter for The Herald-Palladium newspaper in St. Joseph, MI. Portions of this article and some of the photographs, all taken by the author, originally appeared in that newspaper.*

**Human Power: the forgotten energy (ISBN: 0 9536174 1 6) by Arnfried Schmitz, with Tony Hadland**

The last issue of *Human Power*, no. 49, led with an intriguing article by Arnfried Schmitz: "Velocar variations", in which he briefly described around ten recumbents he had built. His biographical note states that he worked in shipbuilding and as a mechanic as a West German student, and later he settled in France and became enthusiastically involved in the HPV movement and its gurus across Europe. He described himself as being known as the "goat-herd from Provence…." Arnfried Schmitz had earlier become known to readers of *Human Power* through his historical authentic (almost an insider's) account "Why your bicycle hasn't changed for 106 years" (vol. 11 no. 3 1994). All this made him something of a mystery man. This small book—128 pages—which he was kind enough to send me, explains a great deal, in a delightfully casual, modest, yet deeply felt way. We learn incidentally that he is a farmer and raises goats, so that explains the "goat-herd" reference. However, almost nothing about him is revealed in the first nine chapters. These are devoted to a fuller re-telling of the history of the early efforts to streamline bicycles and to produce recumbents than I have previously read anywhere. Here are some examples of details of which I wasn't fully aware. "In Berlin the first international race for streamlined bikes takes place." (I believe that was in 1913.) "Charles Mochet sponsors a cup for the absolute hour record for human-powered vehicles regardless of type." (I believe in late 1933 or early 1934). "The Mochets were then professionally building cars and bikes, what we would today call Human-Powered Vehicles… [The] Mochets built mini-cars from 1920 to 1960. They constructed some 6,000 pedal-cars between 1925 and 1944…. They built about 800 [recumbent bikes] between 1932 and 1940." "In 1932 the 'VV' [Velocar] was awarded first prize in the inventors' Grand Prix Lepine for its "indirect steering for recumbent cycles" [using a "universal joint"]. There are also details of how Georges Mochet heard about the Aspo Speed Challenge at Brighton UK in 1980 (stimulated by the annual IHPVA speed championships) and traveled there with a version of the Faure record-breaking Velocar of 1933, but, states Schmitz, no one knew anything about it or the Mochets. But Schmitz read about the races and about those in the U.S.A. in the French bicycling magazine *Le Cycle*, and became excited by the potential. From then on the book becomes partly autobiographical, as he describes how he tried building recumbents, partly for others and partly for himself and his son Jurgen. (He had some difficulty persuading him to ride the machines.) But the details of his and his family's HPV activities often takes a minor role because Arnfried Schmitz gives insightful details of many others. For instance, the complex character of the late Wolfgang Gronen comes alive: he is given a great deal of credit for promoting bicycle and HPV racing in Europe, as well as having a few warts exposed.

Tony Hadland, who has written very fine books on British portable bicycles, on space-frame Moultons and Sturmey-Archer gears, has designed and published this book. It is obtainable from Amazon.com or by direct mail from Arnfried Schmitz, Quartier Gallas, 84220 Lioux Gordes, France: 140 francs, or from Rosemary Hadland, 39 Malvern Road, Balsall Common, Coventry CV7 7DU, UK. In British pounds it is UK £12.95; Europe £13.95 (airmail); rest of the world £14.95 (airmail). The book isn't a dry history book but rather is a living document (written a little strangely in the "historic" present tense), and it isn't precise about everything about which we'd like to know more, but I'm sure that we'll hear again from the author. Every enthusiast for HPVs should read this book.

*Reviewed by Dave Wilson*

## LETTERS

**Supplement to "Velocar variations" by Arnfried Schmitz**

A "key" picture for this article in HP 49 (winter 1999–2000) was unfortunately lost between France and the USA. Here it is, with our apologies. It was published in the French sports press to illustrate the Velodrome d'Hiver event on February 20, 1934 in Paris. This was the very moment that a recumbent was recognised as legal by the Union Cycliste Internationale.

The rider of the Velocar, Francis Faure, was a young well-known track cyclist of the time, but he was certainly far from being a champion. Here he is photographed passing a champion, Henry Lemoine, in the pursuit race.

I want to make another comment on an aspect of bicycling that became more obvious during my riding various bicycles as I was working on the article: riding in a dead straight line is impossible while pedalling, whether on an upright or a recumbent. We ride in a wavy line, as we can see when we have wet tires on a dry road or when we ride in snow. What is wrong with our supposedly perfect machines if they don't want to go straight? Is it because we use our legs alone and don't balance with our arms as we do when walking or running? What do you think?

*—Arnfried Schmitz, Quartier Gallas, Lioux, Gordes, F84220 France, 24 March 2000*



## EDITORIAL

***Ronald van Waveren***

*(translated by Ellen Wilson)*

I'd like to introduce myself to you. I am Ronald van Waveren, 48 years old, father of two grown children and, for four years, chairman of the NVHPV (the Dutch HPV association).

In comparison with many other HPV associations in the world, the NVHPV has grown considerably in the last few years. Perhaps this is thanks to our recumbent-friendly infrastructure—our country is flat, windy and has a lot of bike-paths—and to the increasing use of recumbents in the Netherlands. It is estimated that there are more than 25,000 recumbents here at this time. The NVHPV has almost 1600 members, and recumbent owners and riders represent the largest percentage of members. Originally this was an organization made up of recumbent designers and builders, following the American example. But since the recumbent has now been made available as a serious commercial product through diverse factories, the number of recumbent owners has increased proportionately within the membership. The NVHPV wants to be in the limelight, but its objective should be to stimulate the development and promotion of the use of HPVs in general. And this is constrained by our allegiance to the recumbent.

We organize activities such as presentations at fairs; competitions in the summer and "warm-up days" in the winter; NVHPV annual meetings in association with a number of smaller state-run events; and a large international recumbent-promotional event called Cycle Vision. It is on the topic of this last event that I'd like to ask for your attention. Cycle Vision, for the fourth successive time, will be held early in June, on the weekend of June 3rd and 4th, 2000. It will again be located in Lelystad, on the government's testing grounds for highway vehicles. There will be many activities on this area. A single tent of 1000 $m^2$ can hold all the displays of new products of Dutch and foreign recumbent companies. Under the same "roof" there will be presentations and demonstrations, and a simultaneous second-hand market. If one is interested in a certain vehicle, new or used, one can take test rides on a special adjoining parking lot. Announcements of all events, together with cool music, are broadcast over loudspeakers.

International competitions will be held on the 2700-m test-track with adjacent accommodations. One can enjoy criteriums, 200-m sprints, "devil-take-the-hindmost" drag races, one-hour time trials and a six-hour race. Cash prizes totalling NLG10,000 (over 4500 in US dollars or in Euros) will be given out for all distance races. On this pre-eminently suitable road and in this international framework a real effort was made in an earlier Cycle Vision to break the world hour record (over 80 km/h). For this attempt, foreign teams, among them those from Germany, Britain, Belgium, France and Holland, participated when weather conditions allowed. New this year are the single-class criteriums such as Thys' "Row-Bike", Flevo's "All-Weather" (Allewed-er) and Challenge's "Hurricane".

Cycle Vision is easily accessible by train from Schiphol Amsterdam airport to Lelystad. A bus for Harderwijk will take you to Lelystad airport, and a Cycle Vision shuttle bus will take you the last 3 km. There is also adequate parking. For those who want to visit the event for both days there are overnight camping sites at "The Oppertje." Lelystad also has hotels, B&Bs etc. The price of admission is only NLG7.50 per day. In 1998, Cycle Vision, an organization with more than one-hundred volunteers, attracted 3000 visitors and more than 100 competitors. In 1999 it had 1000 $m^2$ of exposition space, a recumbent-clothing style show; a toddlers' activity area; a children's recumbent trial/obstacle course; 2000 $m^2$ of adult recumbent trial/obstacle course with all of the Netherlands' available recumbents; and the awards for a large design competition, the Bike 2000 Construction Contest (likewise an NVHPV initiative). See www.ligfiets.net for more information.

We Europeans, realizing that a trip to the European continent is not within the reach of every non-European, nevertheless invite all HPV enthusiasts from every part of the globe to take part as competitors or spectators in Cycle Vision 2000, a sensational feast that is a true bike revival. Cycle Vision is an initiative by the Dutch HPV association that has become an annual happening, which you as an enthusiast cannot afford to miss.

---

*Editor's note: Delays to the publication of this issue means that Ronald van Waveren's description of Cycle Vision has come too late to persuade readers to travel there this year, but we hope that a record number will visit this wonderful event next year.*

*—Dave Wilson*

Courtesy Arnfried Schmitz

**Francis Faure passing Henry Lemoine in a UCI-sanctioned pursuit race at the Velodrome d'Hiver in Paris, February 1934.**

**Praise from IHPVA's founder, Chester R. Kyle**

I just got my copy of *Human Power*, and it is one of the best ever—content, photos, graphics, editing, etc. Congratulations. Keep up the good work.
Best Wishes,

Chet

**International Human Powered Vehicle Association**

IHPVA
PO Box 1307
San Luis Obispo, CA 93406 USA
http://www.ihpva.org